AD-A149 350 QUATERNARY NARROW-BAND SEMICONDUCTORS (HGTE)X(INSB)1-X 1/1
FOR FAR-INFRARED DETECORS(U) SAN DIEGO STATE UNIV
FOUNDATION CA L I BERGER ET AL. 31 AUG 84
UNCLASSIFIED N00014-83-K-0588 F/G 17/5 NL

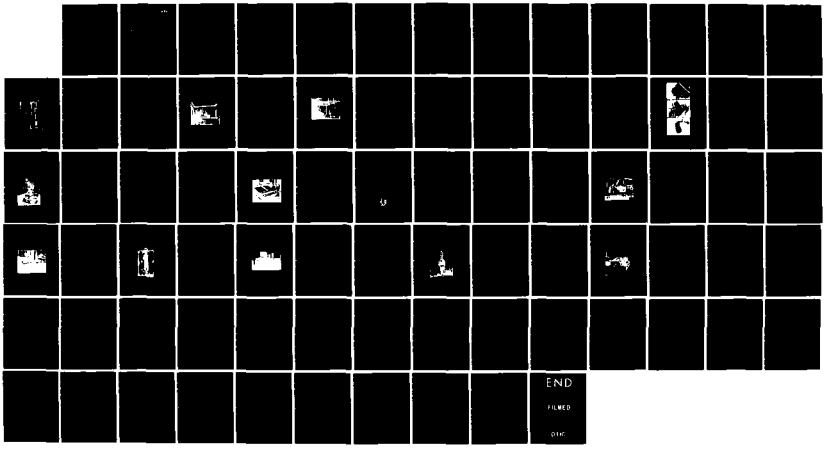

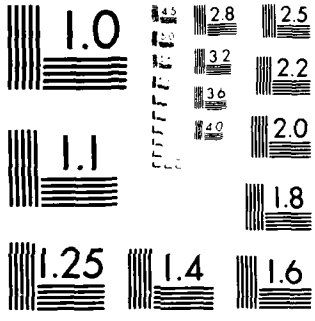

(12)

SDSU FOUNDATION

Quaternary Narrow-band Semiconductors

$(HgTe)_x(InSb)_{1-x}$ for Far-infrared Detectors

Submitted to
Office of Naval Research
by
San Diego State University Foundation

SECURITY CLASSIFICATION OF THIS PAGE (When Data Entered)

REPORT DOCUMENTATION PAGE		READ INSTRUCTIONS BEFORE COMPLETING FORM
1. REPORT NUMBER Annual Report	2. GOVT ACCESSION NO. AD-A149350	3. RECIPIENT'S CATALOG NUMBER
4. TITLE (and Subtitle) Quaternary Narrow-Band Semiconductors $(HgTe)_x(InSb)_{1-x}$ for Far-Infrared Detectors		5. TYPE OF REPORT & PERIOD COVERED Annual Interim Report 9/1/83 to 8/31/84
		6. PERFORMING ORG. REPORT NUMBER
7. AUTHOR(s) Lev I. Berger and Shui-Wai Lin		8. CONTRACT OR GRANT NUMBER(s) N00014-83-K-0588
9. PERFORMING ORGANIZATION NAME AND ADDRESS San Diego State University Foundation 5178 College Avenue San Diego, CA 92182		10. PROGRAM ELEMENT, PROJECT, TASK AREA & WORK UNIT NUMBERS G1153N RR011-07-04 NR 379-061
11. CONTROLLING OFFICE NAME AND ADDRESS Office of Naval Research Arlington, VA 22217		12. REPORT DATE August 31, 1984
		13. NUMBER OF PAGES 74
14. MONITORING AGENCY NAME & ADDRESS(if different from Controlling Office)		15. SECURITY CLASS. (of this report) Unclassified
		15a. DECLASSIFICATION/DOWNGRADING SCHEDULE

16. DISTRIBUTION STATEMENT (of this Report)

DISTRIBUTION STATEMENT A
Approved for public release
Distribution Unlimited

17. DISTRIBUTION STATEMENT (of the abstract entered in Block 20, if different from Report)

18. SUPPLEMENTARY NOTES

19. KEY WORDS (Continue on reverse side if necessary and identify by block number)
Mercury telluride-indium antimonide; Semiconductors; Alloys; Infrared detector; Solid solutions; Mercury Cadmium Telluride

20. ABSTRACT (Continue on reverse side if necessary and identify by block number)

This annual report includes a description of results from work on investigation of the quaternary system $(HgTe)_x(InSb)_{1-x}$ in accordance with Project N00014-83-K-0588 during the first year from September 1, 1983 to August 31, 1984.

In the course of this time period, the special furnaces for synthesis of the polycrystalline specimens in the system HgTe-InSb were made, the optimal ampules for synthesis and differential thermal analysis were

DD FORM 1 JAN 73 1473 EDITION OF 1 NOV 65 IS OBSOLETE
S N 0102-LF-014-6601

SECURITY CLASSIFICATION OF THIS PAGE (When Data Entered)

20. ABSTRACT (continued)

designed, and the appropriate equipment for the specimen assessment was bought or adjusted. On the basis of the results of several first cycles of synthesis, the temperature-time regime for single-phase polycrystal synthesis was developed. The single-phase ingots were synthesized with the vast range of composition, but the primary interest was concentrated upon synthesizing the single-phase specimens in the part of the concentration diagram which contains semiconductor alloys from 100 to 80 mole % InSb where the absorption edge range from 7 μm to 12 μm is expected.

Synthesized specimens were used for microstructure analysis, differential thermal analysis (DTA) and x-ray analysis. Measurements of microhardness were used to proof the single-phase structure of the specimens. The alloy specimen assessment included also electrical, galvano-magnetic and optical measurements in the IR part of the spectrum.

Measurements of the electrical transport properties have shown that all synthesized specimens have n-type conductivity with the magnitude of electrical resistivity close to 10^{-3} ohm.cm. As is typical for polycrystals, magnitude of resistivity depends mainly upon the electron wave dissipation from the grain boundaries.

Measurements of optical transmittance and reflectance in the IR part of the spectrum produced the information regarding the edge of the absorption band as the function of composition in the polycrystalline samples.

The sum of the results is used to develop the phase diagram of the semiconductor part of the $(HgTe)_x(InSb)_{1-x}$ system, the diagrams composition-property for lattice parameters, concentration and mobility of the current carriers, and for the absorption edge in the infrared part of the spectrum.

The main purpose of this project is the development of growth techniques for crystals and epitaxial layers of $(HgTe)_x(InSb)_{1-x}$. The goal is to synthesize and evaluate single crystals and/or epitaxial films of these substances and provide recommendations for their use as materials for far-infrared photoresistive and photovoltaic detectors.

ANNUAL REPORT

PROJECT TITLE: QUATERNARY NARROW-BAND SEMICONDUCTORS $(HgTe)_x(In\ Sb)_{1-x}$ FOR FAR-INFRARED DETECTORS

GRANT NO: N00014-83-K-0588

PRINCIPAL INVESTIGATOR: LEV I. BERGER
DEPARTMENT OF PHYSICS
San Diego State University
(619)265-6163/6240

SUBMITTED TO: OFFICE OF NAVAL RESEARCH
ARLINGTON, VIRGINIA 22217

STARTING DATE: SEPTEMBER 1, 1983

REPORTING PERIOD: SEPTEMBER 1, 1983 - AUGUST 31, 1984

COMPLETION DATE: AUGUST 31, 1986

Lev I. Berger

LEV I. BERGER
PRINCIPAL INVESTIGATOR

Table of Contents

ABSTRACT

This annual report includes a description of results from work on investigation of the quaternary system $(HgTe)_x(InSb)_{1-x}$ in accordance with Project N00014-83-K-0588 during the first year from September 1, 1983 to August 31, 1984.

In the course of this time period, the special furnaces for synthesis of the polycrystalline specimens in the system HgTe-InSb were made, the optimal ampules for synthesis and differential thermal analysis were designed, and the appropriate equipment for the specimen assessment was bought or adjusted. On the basis of the results of several first cycles of synthesis, the temperature-time regime for single-phase polycrystal synthesis, was developed. The single-phase ingots were synthesized with the vast range of composition, but the primary interest was concentrated upon synthesizing the single-phase specimens in the part of the concentration diagram which contains semiconductor alloys from 100 to 80 mole % InSb where the absorption edge range from 7 μm to 12 μm is expected.

Synthesized specimens were used for microstructure analysis, differential thermal analysis (DTA) and x-ray analysis. Measurements of microhardness were used to proof the single-phase structure of the specimens. The alloy specimen assessment included also electrical, galvano-magnetic and optical measurements in the IR part of the spectrum.

Measurements of the electrical transport properties have shown that all synthesized specimens have n-type conductivity with the magnitude of electrical resistivity close to 10^{-3} ohm cm. As is typical for polycrystals, magnitude of resistivity depends mainly upon the electron

wave dissipation from the grain boundaries.

Measurements of optical transmittance and reflectance in the IR part of the spectrum produced the information regarding the edge of the absorption band as the function of composition in the polycrystalline samples.

The sum of the results is used to develop the phase diagram of the semiconductor part of the $(HgTe)_x(InSb)_{1-x}$ system, the diagrams composition-property for lattice parameters, concentration and mobility of the current carriers, and for the absorption edge in the infrared part of the spectrum.

The main purpose of this project is the development of growth techniques for crystals and epitaxial layers of $(HgTe)_x(InSb)_{1-x}$. The goal is to synthesize and evaluate single crystals and/or epitaxial films of these substances and provide recommendations for their use as materials for far-infrared photoresistive and photovoltaic detectors.

The continuation of this project includes:

-single crystal growth,

-thin film growth by vapor phase epitaxy,

-Laue and Debye-Scherrer analysis of the single crystals and films,

-measurements of electrical conductivity and Hall effect,

-measurements of the optical parameters,

-manufacturing and investigation of infrared detector models.

The Bridgman-Stockbarger method will be used for crystal growth, and the so-called EDRI method (evaporation-diffusion at isothermal conditions) will be used for vapor-phase epitaxial growth. The electroreflectance method will be used for optical measurements in the visible part of the spectrum. Absolute black body measurements will be used in the infrared part of the

spectrum. Measurements of electrical, galvano-magnetic and thermoelectric properties have been included in the project to provide information on the band structure of the quaternary materials. Thermal conductivity and thermal expansion data for infrared device technology purposes will be obtained by using new methods of measurement. Two patents on the thermal conductivity and thermal expansion measurement methods will be pending.

The main results of this work will be the introduction of a new group of semiconductor materials into the infrared detector technology for wavelengths greater than 6μm.

ANNUAL REPORT

1. INTRODUCTION

This report includes results of the first year of investigation of the alloys in the quaternary system HgTe-InSb. A relatively small difference between the energy gap magnitudes of the binary components, low melting point of indium antimonide and its comparatively big microhardness have led to the conclusion that electro-optical as well as technological characteristics of the quaternary alloys are superior to mercury-cadmium telluride.

The reported year schedule included as a main part the synthesis of single-phase alloys and investigation of their physicocheical properties; first of all the lattice structure, lattice parameters, phase relations in the alloy system, microstructure and microhardness of the alloys. The galvano-magnetic investigation of the compositional dependence of sign, concentration and mobility of the current carriers in the polycrystalline samples served mainly as an auxiliary method of phase analysis of the alloys. The optical measurements were used for evaluation of the range of existence of semiconductors in the quaternary system, and for investigation of energy gap-composition relation.

The sum of the experimental result is used to develop the phase diagram of the $(HgTe)_x(InSb)_{1-x}$ system and the diagrams composition-property. The sum of the results of the first year of work on this project is a reliable basis for the growth of crystals and/or epitaxial layers with the chosen

electro-optical characteristics. From our point of view, the most economical and effective method of crystal growth for this pseudobinary system is the Bridgman-Stockbarger method. There is reason to believe that the geometry of the sharp end of the ampule for crystal growth plays a role equally important to the temperature gradient and rate. We are planning to conduct a series of experiments to determine the shape of the space inside of the ampule upon the process of crystal growth.

A variant of the vapor phase epitaxy will be used for thin single crystalline layer growth. We plan to use the so-called EDRI (evaporation-diffusion under isothermal conditions) method.

All crystals and epilayers will be used to investigate the correlation between the parameters of growth (time, temperature, its gradients, rate of its change, geometry of the crystalization vessel, etc.) and fundamental electrical and optical properties; namely, sign, concentration and mobility of current carriers, cut-off wave length, composition of material, crystallographic orientation, etc.

The main objective of the program is to fabricate new intrinsic semiconductor materials for use as infrared detectors with significantly improved optical and electro-optical parameters, especially, better photoresponse time, by use of the binary components with the highest known mobility and the smallest effective mass; better cut-off wavelength resolution by using solid solutions with relatively small composition dependence of energy gap; and better detector long-term stability, as a result of the relatively small change in electro-optical properties with a

change of composition due to sublimation of the volatile components from the surface of the detecting crystal or thin film.

The work of the reported year was done in accordance with the schedule (see Table 1)

2. EXPERIMENT

2.1. SYNTHESIS OF ALLOYS

The alloys were synthesized from the powder of the binary components in the evacuated and sealed quartz ampules. A definite amount of mercury was added to the ampules to prevent decomposition of HgTe in the process of synthesis. To avoid loss of material in the process of specimen preparation we used ampules with flat bottoms (see Fig. 1.) The ampules were made from quartz tubing 3 mm thick to prevent explosions at elevated temperatures. The method of stepped heating and cooling was used for synthesis. Thermolyne tube furnaces and the Norman Kiln muffle furnaces were used for synthesis. For stabilization of the synthesis parameter; first of all, time derivative of temperature, a special high inertia furnace was made (see Fig. 2), that has also a very small temperature gradient in the working volume.

The procedure of purification of ampules for loading consists of steps presented in Table 2.

The ampules are evacuated to the residual pressure <15 mPa and sealed on the vacuum stand (Fig. 3). To prevent sublimating the sample during the process of sealing the quartz ampule, we grind the quartz rod facing the sample and cool the sample part of the ampule in ice-water bath. The quartz tubing and rods used are products of GM Associates, Inc.

TABLE I. SCHEDULE OF THE PROGRAM

Investigation of the Quaternary Narrow-band Semiconductors $(HgTe)_x(InSb)_{1-x}$ for Far-infrared Detectors	Months Following Contract Award
	2 4 6 8 10 12 14 16 18 20 22 24 26 28 30
Part I:	
1. Single-phase sample preparation	
2. Differential thermal analysis	
3. X-ray analysis	
4. Electrical conductivity and Hall effect	
5. Measurements of optical parameters	
6. Annual report	
Part II:	
1. Single crystal growth	
2. Thin films grow by VPE	
3. X-ray analysis	
4. Electrical conductivity and Hall effect	
5. Measurements of optical parameters	
6. Annual report	
7. Correction of methods of sample and p-n transition preparation	
8. Manufacturing and investigation of the models of infrared detectors	
9. Final report	
	2 4 6 8 10 12 14 16 18 20 22 24 26 28 30

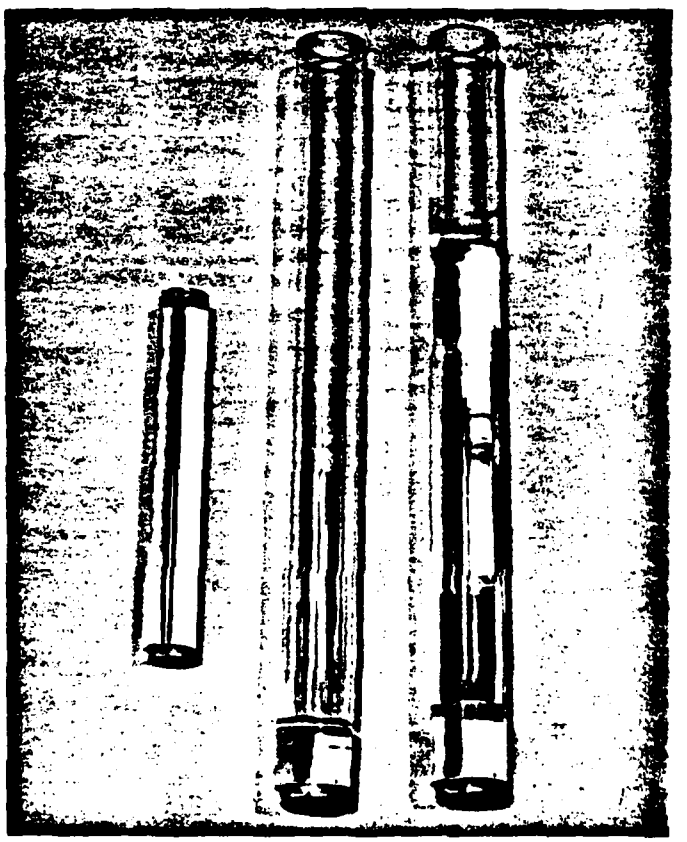

Fig. 1. A typical sealed quartz ampule for synthesis of $(HgTe)_x(InSb)_{1-x}$

The temperature-time profile of polycrystals synthesis depends upon the content of the atomic % of HgTe in $(HgTe)_x(InSb)_{1-x}$. The highest temperature in the synthesis of low atomic % of HgTe (2 to 10%) polycrystals can be set as low as 600°C, while at high atomic % of HgTe it is 720°C. The detail of the synthesis for each group of polycrystals will be given later in this report.

The chief characteristics of solid solutions in a majority of tetrahedral semiconductors is that their mixing energy is extremely small. All diffusion processes in liquid and solid state are very slow. There are two ways to accelerate the solubility process; namely, (i) increase the temperature at which the process takes place, and (ii) use vibration of the melt.

In the case of mercury containing alloys the temperature increase will be followed by mercury evaporation and by an increase in the vapor pressure inside of the quartz ampule.

From the data [1,2] vapor pressure of mercury upon HgTe at 700°C (30° higher the HgTe melting point) is about 1.5 MPa. This magnitude is much smaller than the mercury vapor pressure upon liquid mercury which is 6.4 MPa at this temperature [3]. Because of these magnitudes we did not increase the temperature above 700°C and tried to use the so-called stepped heating synthesis regime [4]. The purpose of this regime is to keep as large an amount of mercury as possible in the bounded state. In the case of the $(HgTe)_x(InSb)_{1-x}$ system this method has an additional advantage. It is known (see, for example [5]) that HgTe is an unstable compound and it starts to decompose at temperatures higher than 500°C. The same takes

TABLE 2. PURIFICATION OF QUARTZ AMPULE

	Solution	Remarks
(1)	Aqua-Regia	4 hours immersion
(2)	Deionized water	50 washing cycles
(3)	Acetone	5 washing cycles
(4)	Deionized water	10 washing cycles

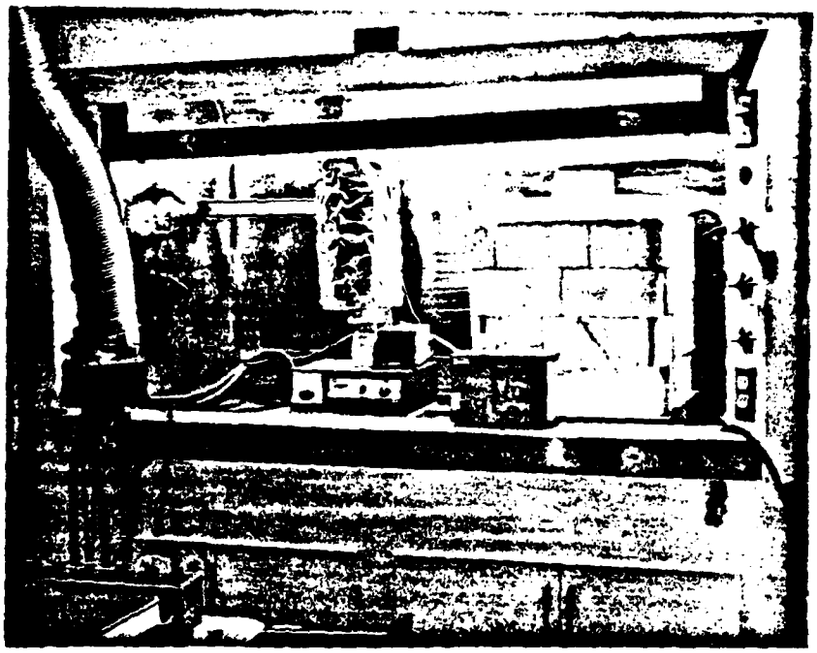

Fig. 2. The high inertia furnace used in synthesis of polycrystals of $(HgTe)_x(InSb)_{1-x}$

place with InSb in the melt [15]. This means that at these temperatures (but below the HgTe melting point), in the ampule containing binary compounds InSb and HgTe, we may have liquid InSb, solid HgTe and free Hg and Te in the gas phase. The results of experiments [6,7] indicated that we could expect that InSb with low partial pressure of its components might serve as a matrix for mercury and tellurium atoms of the vapor phase. During the process of cooling the liquid solution, atoms (or molecules) of Hg and Te connect themselves to the surface of the melt and diffuse in the volume of liquid.

We are synthesizing $(HgTe)_x(InSb)_{1-x}$ alloys from the binary components* in the thick-wall quartz ampules. To prevent mercury losses in the process of synthesis we add metallic Hg in the initial mixture. The amount of Hg is calculated upon the basis of kinetic theory of gases. In our experiments we strive to minimize the free volume of the ampule. For this purpose we do not seal the ampule itself but insert a quartz rod with a diameter slightly smaller than the inner diameter of the ampule up to the surface of the mixture of components, evacuate the ampule, and seal the wall of the ampule to the surface of the rod. This prevents evaporation of substantial amounts of the volatile components and helps keep the initial mixture at a low temperature at the time of sealing. To prevent the ampule from explosion we use quartz tubing with a wall 3 mm thick.

*Binary compounds were made by Poly Research Corp. (InSb-99.999%, HgTe-99.99%

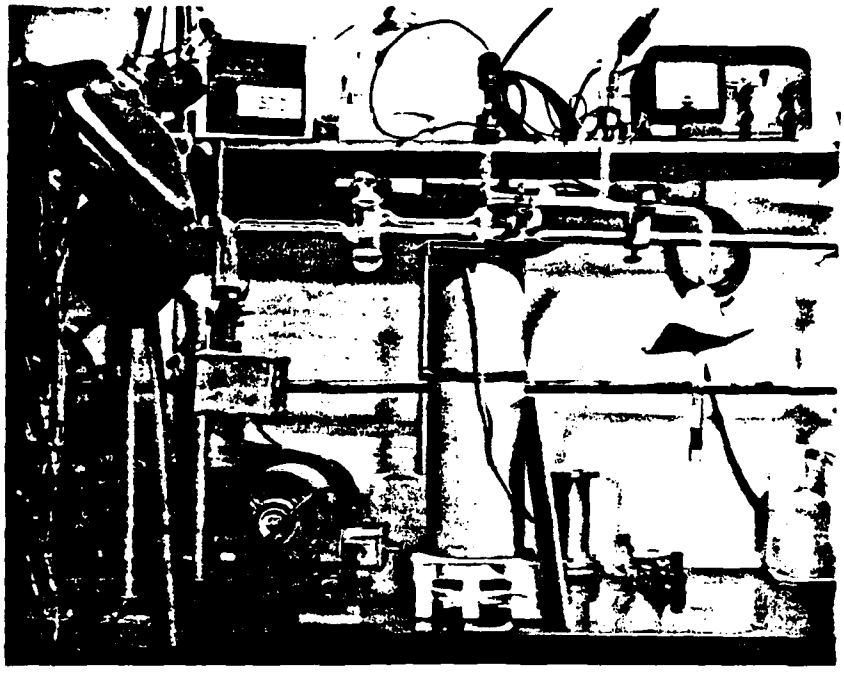

Fig. 3. Vacuum line for sealing the quartz ampule

During the reported period we had 47 cycles of synthesis of the HgTe-InSb alloys. The composition of a part of alloys is presented in Table 3.

The last step in the process of synthesis included annealing and quenching of the specimens in water. In some cases we quenched specimens from the highest temperature (720°C) to determine whether the atoms in the melt had the same (tetrahedral) short range order as in the solid state. In all experiments with semiconducting alloys we did not discover decomposition of the alloys during the phase transition liquid-solid. It is possible to say that 720°C is a relatively low temperature for the liquid HgTe (compare with temperatures of the order of 1000°C in HgCdTe technology) and decomposition of HgTe apparently does not take place.

X-ray analysis of the specimens being quenched from different temperatures did not show any sign of the existence of rhombohedral and tetragonal (Hg, In, Sb) or trigonal (Te) peaks which is in accordance with the results of the microstructure analysis.

As was mentioned before, for the reported year, we performed a total of 47 preparations of $(HgTe)_x(InSb)_{1-x}$ in the range of HgTe content from 2 to 80 atomic percent and at various heating sequences. The preparations can be divided into 3 groups depending on the atomic percentage of HgTe in $(HgTe)_x(InSb)_{1-x}$; they are:

Group I. Sample containing from 2 to 12% in HgTe

Group II. Sample Containing from 12 to 20% in HgTe

Group III. Sample with HgTe content greater than 20%

The preparation of each group of samples is summarized below:

TABLE 3. COMPOSITION OF SOME SYNTHESIZED SPECIMENS

Sample	Composition				Free Hg Content, mg
	InSb		HgTe		
	mole %	weight %	mole %	weight %	
1	98	97.25	2	2.75	1.6
2	95	93.20	5	6.80	1.6
3	90	86.64	10	13.36	1.6
4	88	84.09	12	15.91	1.7
5	85	80.33	15	19.67	1.6
6	80	74.25	20	25.75	1.9
7	60	51.95	40	48.05	1.7
8	40	32.46	60	67.54	1.8
9	20	15.27	80	84.73	1.5

Group I (2 to 10% in HgTe):

For each preparation, 10 grams of HgTe and InSb was ground into powder form and mixed well before loading into the bottom of a clean thick wall quartz ampule through a conveying glass tubing. This kept the upper ampule wall clean. The powder was then packed by vibration. A small droplet of Hg was introduced onto the packed sample, the weight of Hg used was based upon the free volume produced when the powdered sample was melted. Finally, a quartz rod was inserted into the quartz ampule, and the sample was packed again by applying pressure at the end of the quartz rod. The ampule was then sealed with a hydrogen-oxygen torch under vacuum. In order to prevent damaging the sample due to heating during the sealing process, the end of the quartz rod facing the sample was polished and the end of ampule containing the sample was cooled in ice-water bath. The sealed ampule was placed in a well insulated box furnace. The heating sequence was the following:

24 hours at 300°C

120 hours at 600°C

48 hours at 300°C

The samples were cooled in the furnace with the power off. They appeared to be a single solid ingot.

Group II (>12 to 20% in HgTe)

The preparation procedure of the sample was the same as stated in Group I except for the heating and cooling process. The heating sequence was the following:

1 hour at 500°C

1 hour at 720°C

240 hours at 500°C

3 hours at 720°C

24 hours at 500°C

The samples appeared to be single solid ingots.

Group III (>20 to 80% in HgTe):

The preparation procedure of the sample was stated in Group I with the exception of the heating and cooling process. The heating sequence was the following:

24 hours at 300°C

96 hours at 720°C

24 hours at 500°C

24 hours at 300°C

The samples were cooled in the furnace with the power off.

The resultant sample contained more foam structure inside the ingot as the percentage of HgTe increased in each sample. This may have been due to the unreacted HgTe distributed inside the ingot. The DTA indicated there was more than one phase in these preparations.

2.2. SPECIMEN ASSSESSMENT

The specimen assessment includes phase analysis, microstruture and microhardness evaluation, analysis of crystal structure and lattice parameter measurement, electrotransport and galvanomagnetic properties investigation, and measurement of infrared transmission and reflection. This information is a necessary minimum for the semiconductor polycrystal sample description

2.2.1. MICROSTRUCTURE ANALYSIS

For microstructure analysis, specimens were molded into Epo-Kwick epoxy resin cylinders and polished mechanically with 0.05 micro powder of gamma aluminum. Polished specimens were etched in 1 to 2 dilution of 2:1:1 parts of concentrated HNO_3, HF and HAC respectively. The photos of the specimens' micro structures are presented in Fig. 4*. One can see single-phase grains with the average size of about 1 mm and also twins in the field of vision. Tendency for the twin creation is very typical for alloys both on InSb and HgTe basis. In some cycles of synthesis we were able to find spherical cavities filled with mercury (so called pinholes). These pinholes are very typical for HgCdTe, but in our experiments they could be observed only in the runs where specimens were quenched in water from the highest temperatures. We believe that these pinholes are the consequence of the existence of excess mercury in comparison with the stoichiometric composition. In the process of fast

(a)

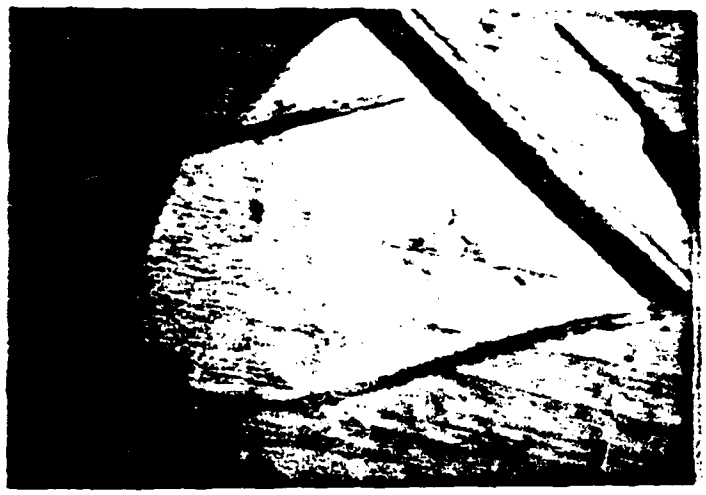

(b)

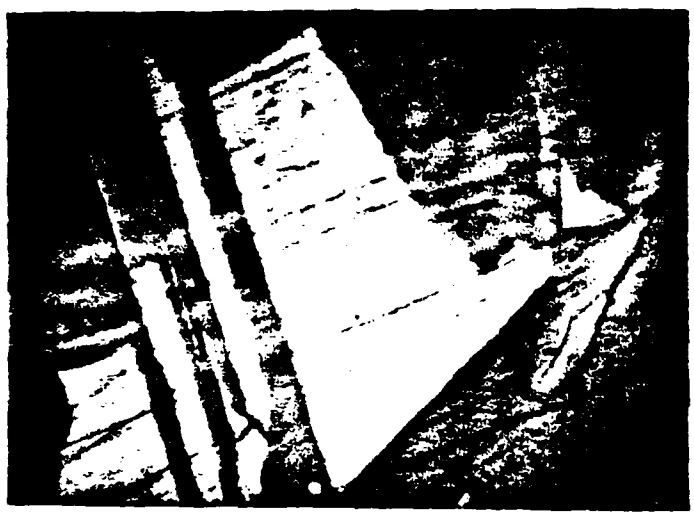

(c)

Fig. 4. Microstructure of two HgTe-InSb specimens.
(a) 98% Insb, 2% HgTe, magnification 100X
(b) 95% InSb, 5% HgTe, magnification 100X
(c) 90% InSb, 10% HgTe, magnification 100X

crystallization this mercury does not have enough time to migrate to the surface of the grains or to the surface of the specimen. We did not see the mercury pinholes in the specimens which were annealed at the temperatures slightly below the solidus points. This fact provides one more piece of evidence about the advantage of $(HgTe)_x(InSb)_{1-x}$ alloys in comparison with HgCdTe ones.

2.2.2. MICROHARDNESS MEASUREMENT

Microhardness measurements were undertaken to prove the existence of only one phase of the specimen on the microscopic level, because x-ray analysis cannot identify a phase if its content is smaller than 5% [9]. On the other hand, difference in light absorption for different wavelengths and in different crystallographic directions quite often gives an illusion of the presence of more than one phase in the field of vision of a microscope during the microstructure analysis. In the case of the HgTe-InSb alloys the microhardness method is especially convenient for the phase identification because the binary components have significantly different microhardnesses (220 kgp/mm^2 for InSb and 30 kgp/mm^2 for HgTe [10,11]). The size of the impression in our experiments was about 40 μm. This means that we could identify points of the sample surface at the distance of about 100 μm without a decrease in the accuracy of the experiments. For the microhardness measurements we used a Leitz

Microhardness Meter from Wetzlar, Germany (Fig. 5). In our experiments, the load 0.05 kgp was used. All investigated samples had a relatively small dispersion of magnitudes of microhardness along the surfaces of the specimens. The microhardness data are presented in Table 4.

In accordance with theory [12], our experiments showed a dependence of microhardness on the grain size when the latter is comparable with the diagonal of the impression.

The experimental error in the microhardness measurements, calculated on the basis of the partial derivative method was equal to 2.5% without taking into consideration the ambient temperature fluctuations.

2.2.3 DIFFERENTIAL THERMAL ANALYSIS (DTA)

A special furnace was designed for DTA. The need for this furnace was conditioned by the fact that at high temperatures (around 1000^{o}C) the vapor pressure in the measuring vessel may reach 10 MPa if the binary components decompose at these temperatures. The ampule with an alloy to be investigated and the ampule with a standard material (we use tin) are inserted in the cylinder block which is installed in the furnace (Fig. 6). The internal volume of the furnace is filled with soft refractory brick which is used as a protective sheath. The latter will also absorb the energy of the blast wave in the case of ampule explosion. The sample block was fabricated from stainless steel. The advantage to the use of the

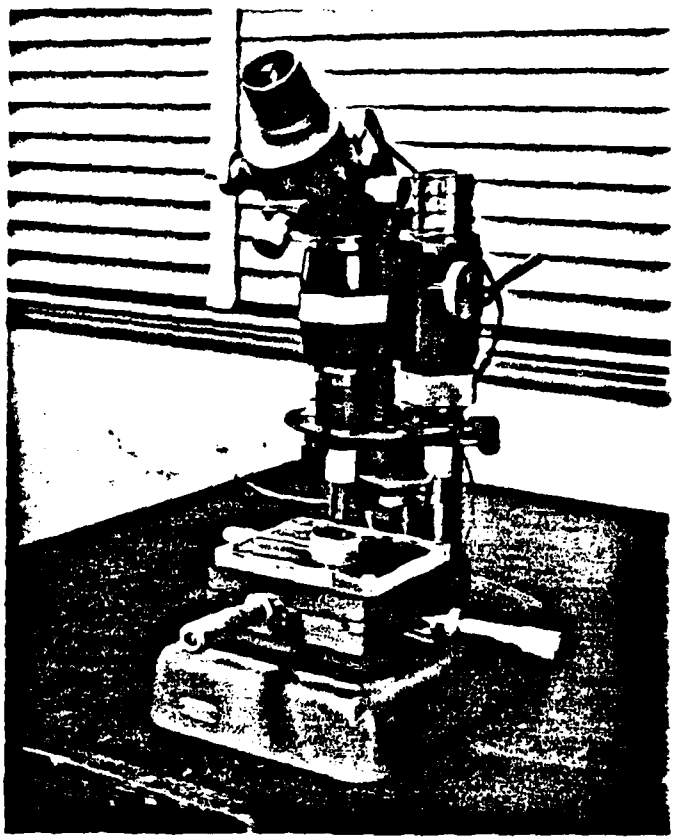

Fig. 5. Reichest Microscope Model No. 328061 used for microhardness tests

metallic block is that it gives rise to base-line drift [16]. The use of tin as a reference material has several advantages; namely, (a) its equlibrium solid-liquid transition temperature (231.9^{o}C) and extrapolated onset temperature (230 $\pm 5^{o}$) are very reliable [17], (b) after first cycle of melting and crystallization in an evacuated and sealed ampule the tin ingot has very high thermal conductivity (0.64W/cm degree[19]) and (c) specific heat of tin is known with high accuracy (0.0530 [18]), which permits calculation of the most suitable amount of material for the reference ampule.

Because of the relatively low melting point, T_m, of tin, each recorded DTA curve had a very sharp peak at T_m which permitted us to check the temperature measurement accuracy after each run of DTA. The ampules were made from 3 mm thick quartz tubing. To raise the sensitivity of our DTA device we designed the ampule with a deep canal for the thermocouple junction and with minimal free internal volume (Fig. 7). In spite of great wall thickness of the quartz tubing the designed ampule permitted the identification of minute thermal effects which could not be observed in the convenient ampules [8] if they were made from commonly used 1 mm thick tubing.

As an example, the thermogram from the sample 88% InSb 12% HgTe (Hewlett-Packard x-y recorder 7.035 B was used) is presented in Fig. 8. The differential curve is typical for a solid solution. There are no effects in the solid state as well as in the liquid state up to 700^{o}C.

The accuracy of the temperature evaluation calculated by the partial derivative method is equal to 2%.

TABLE 4. RESULTS OF THE MICROHARDNESS MEASUREMENTS

Sample No.	Composition, mole % HgTe	InSb	Microhardness kgp/mm^2	Dispersion %
1	0	100	201	5
2	2	98	232	7
3	5	95	238	7
4	10	90	244	5
5	12	88	215	5
6	15	85	201	6

2.2.4. X-RAY ANALYSIS

X-ray analysis was performed on the computer equipped X-ray diffractometer DTM 1057 of Diano Corp. (Fig. 9). The Debye-Scherrer method was used. All measurements were made at room temperature without the sample temperature stabilization. The diffractometer recorder has the accuracy of 1%. The measurements were performed at the angles from 2^{o} to 60^{o} at the rate 2^{o}/min. The main purpose of this stage of experiments was the identification of the crystal syngony and lattice constant.

More precise measurement of the lattice parameters is a part of our plan of the single crystal and epitaxial layer assessment. The same equipment will be used, but X-ray analysis will be performed at large angles (the so-called back shooting). An example of X-ray diffractogram is presented on Fig. 10.

2.2.5. ELECTRICAL CONDUCTIVITY AND HALL EFFECT

For electrical conductivity measurements we used two methods: (a) the so-called collinear four-probe array probe *[13] and (b) the Van-der-Pauw method [20]. Conductivity, in the case of four equidistant probes, is equal to

$$\sigma = \frac{1}{2\pi s} \cdot \frac{I}{V} \qquad (1)$$

where s is the distance between neighboring probes, I is the current between the two outer probes and V is the voltage drop between the inner probes. This measurement in our laboratory can be done only at room temperature. Its accuracy depends mainly upon the accuracy of the used galvanometer. The partial derivative method gives accuracy in the range

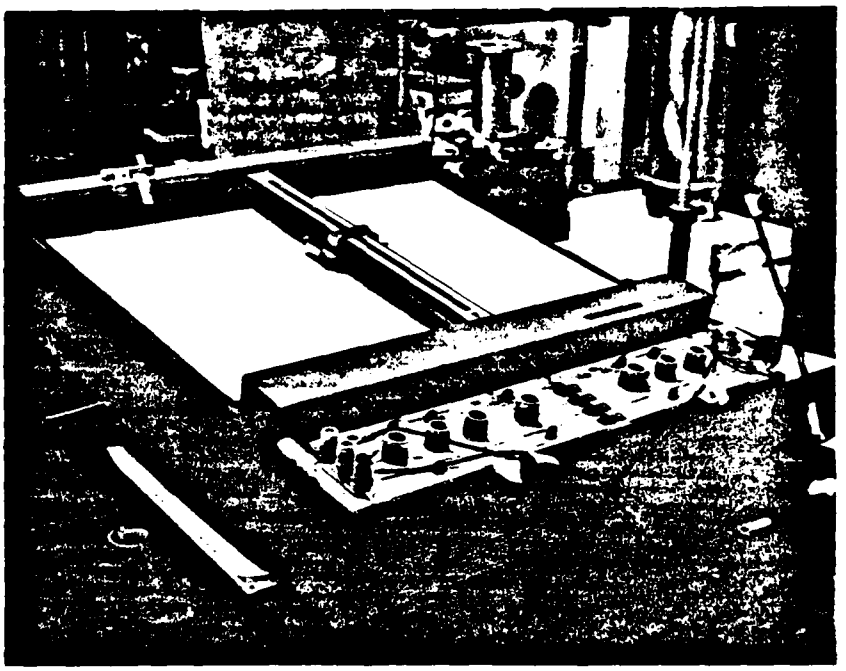

Fig. 6. Apparatus used for differential thermal analysis

3-6% depending on the sample bulk and surface electrical conductivity and, hence, the magntidues of I and V. For conductivity of a lamellae of arbitrary shape, with four probes at different distances between them and arbitrary angles under which one of the probes "sees" its neighbors, calculations [20] give the formula:

$$\sigma = \frac{x.\delta}{\ln^2}\left[\frac{R_{12,34} + R_{23,14}}{2} f(r)\right]^{-1} \qquad (2)$$

where σ is the thickness of the lamellae;

$R_{12,34} = \frac{V_{12}}{I_{34}}$; $R_{23,14} = \frac{V_{23}}{I_{14}}$; V_{12} and V_{23} are voltage drops between probes #1 and 2 or 2 and 3 when current I_{34} or I_{14} is directed between probes 3 and 4 or 1 and 4, respectively. The f(r) is a numerical function of the ratio $r = R_{12,34}/R_{23,14}$:

r =	1	2	5	10	20	50	100	200	500	1000
f(r) =	1	0.96	0.82	0.7	0.59	0.47	0.40	0.35	0.30	0.26

Our measurements were undertaken in the temperature range 77K - 300 K. To double check our results we asked Dr. Clawson of NOSC to measure and Hall effect on our specimens. The results of our measurements are in satisfactory accordance (the difference is not greater than 30%). This difference may be explained by a difference in the contact geometry and the existence of different adsorption layers on the specimen surfaces in two

*Sample holder was manufactured by A & M Ltd., England (Type Rig, Model C)

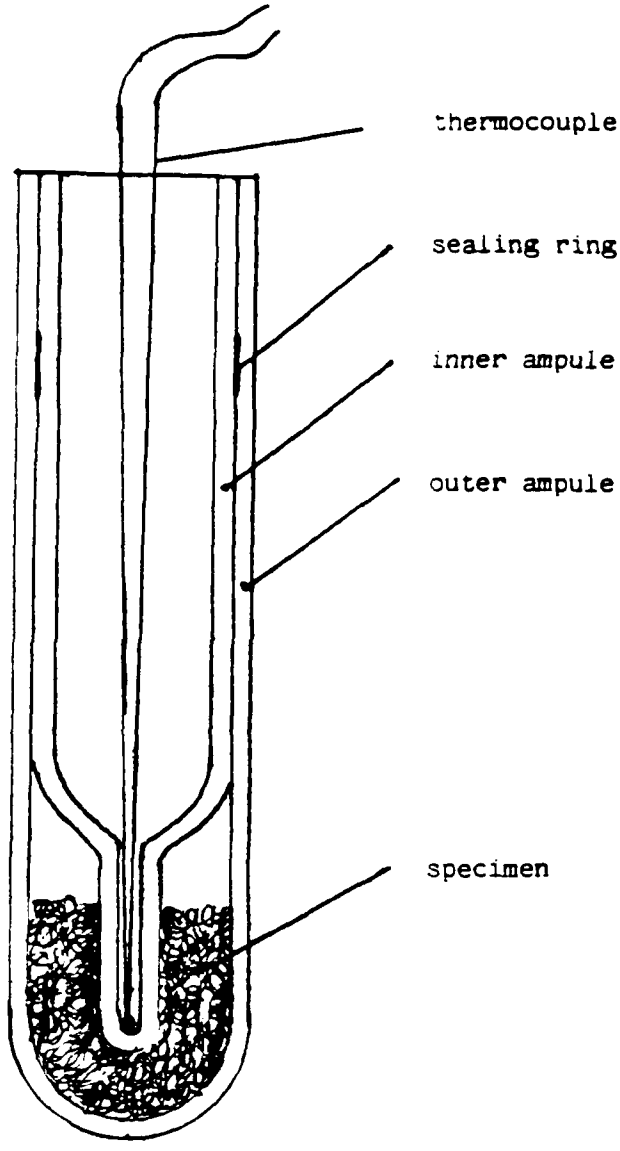

Fig. 7. Ampule used for differential thermal analysis

experimental cycles. As is well known, both InSb and HgTe have extremely high free electron mobility (10^5 and 10^4 $cm^2/V.$ sec, respectively). Estimation of σ at reasonable electron concentration $n = 10^{17}cm^{-3}$ gives $\sigma = neu = 10^{17}cm^{-3} \times 1.6 \times 10^{-19}C\ 10^5cm^2/V.sec = 1.6 \times 10^3(ohm\ cm)^{-1}$. Using formula (2) we have at $I = 10^{-3}A$ and $\delta = 0.5mm$ magnitude $V = 1\mu V$. This means that the conductivity measurements include measurements of the voltage drop at the limits of sensitivity of the available potentiometers. Our σ measurements consequently have a relative error close to 15%. This is a high enough accuracy for the initial measurements of the concentration dependence of conductivity, but not enough for measurements of the temperature dependence of conductivity and Hall effect on single crystals and epitaxial films which will be included in our project for the second year of work. We are designing now a new device which will be used for these measurements.

Our measurements with the four-probe array gave the order of magnitude of $\sigma\ 10^3 - 10^4\ 1/\Omega \times cm$ for the polycrystal specimens, but we could not find a definite correlation between the specimen composition and σ. This result is very typical for polycrystalline specimens, where dissipation of the electron waves takes place mainly on the grain boundaries.

For determination of the sign of the dominant charge carriers (type of conductivity) we use the commonly known thermoelectric probe method with a temperature difference between the probes of about 50^oC. All synthesized specimens have had n-type conductivity. These results show, as can be concluded from formula [14]

$$\sigma = e(\mu_n\ n + \mu_p\ p)_3$$

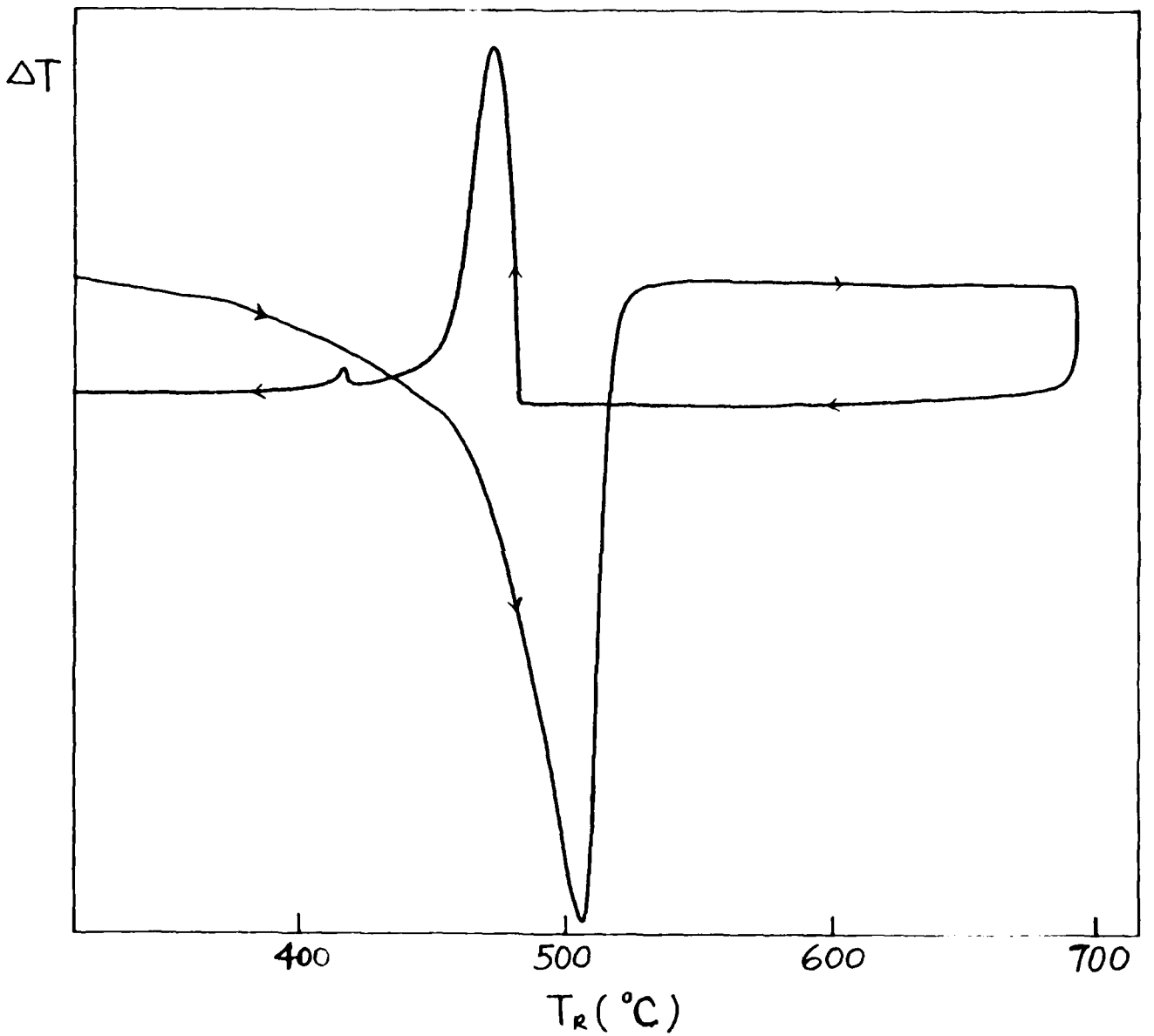

Fig. 8. The differential thermal analysis for the alloy of 88% InSb and 12% HgTe (heating rate = 3°/min; cooling rate = 1°/min.)

where n and p are the electron and hole concentrations respectively, that p in our specimens is the same order of magnitude with n or smaller because the hole mobility μ_p in both InSb and HgTe is about 1% of the electron mobility μ_n. More details about μ_n, μ_p, n and p will be known after we undertake measurements of the electrical conductivity and Hall effect of our alloys in wide temperature range, in combination with the thermoelectric effect and magnetoresistance measurements. As was mentioned before, these results would have a principal value if they were received on single crystals or epitaxial films. However, these measurements will be undertaken only during the second year of work with this project. The Hall effect measurements were undertaken on the Varian Associate V6060 magnet system (see Fig. 11). The measured magnitude of magnetic induction B_z was equal to 15 kG. Induction gradient measurements showed that the magnitudes of $\Delta B_z / x$ and $\Delta B_z / \Delta y$ were below the sensitivity threshold of the measuring instrument used. The accuracy of the Hall measurement was about 15%. The Hall effect at liquid helium temperature will be measured in the near future with the dewar shown in Fig. 12.

2.1.6. INFRARED TRANSMISSION AND REFLECTION

The IR transmission and reflection of photons were used for a determination of the absorption edge; in other words, the energy gap for the alloys. It is known that fundamental band-edge absorption (see, for example, [22,23]) for a direct allowed transition between simple parabolic valence and conduction bands is described by equation

$$\alpha = \frac{A(n)}{hf} (hf - E_g)^{1/2} \qquad (3)$$

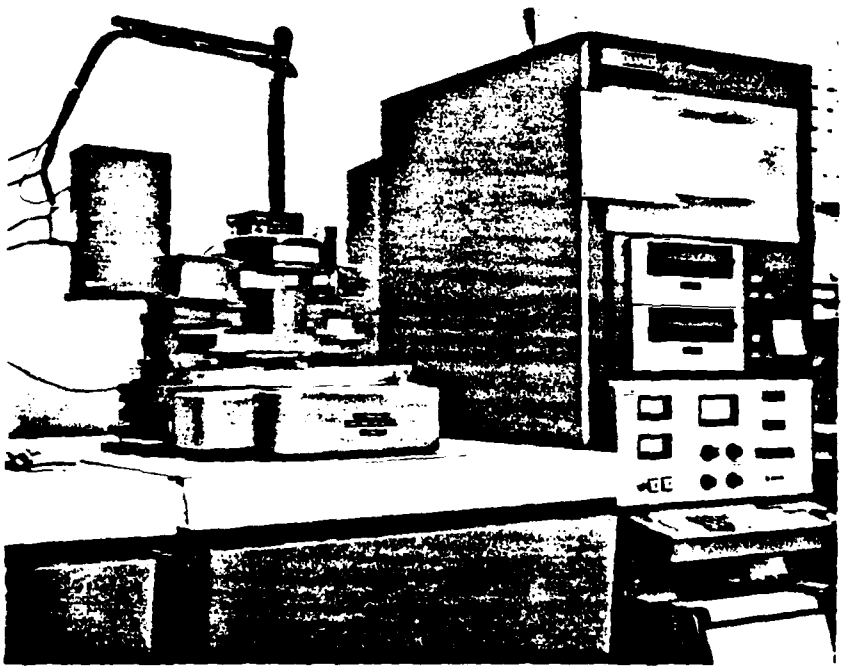

Fig. 9. X-ray diffractometer

where α is the absorption coefficient, A(n) is a parameter which depends upon the band structure and index of refraction, hf is the incident photon energy and ε_g is the energy gap. If we assume n to be a constant, then Eq. (3) can be rewritten in the form

$$hf = \varepsilon_g + C(\alpha hf)^2 \qquad (4)$$

One can see from Eq. (4) that if we plot quantum energy vs. the square of the product hf we will have a straight line. Its intersection with the ordinate axis yields the energy gap.

If we write the Bouguer-Lambert law in the form

$$T = (1-R)\exp(-\alpha x) \qquad (5)$$

where T, R and x are the specimen transmittance, reflectance and thickness respectively, α can be calculated from the results of measurements of T, R and x in compliance with expression

$$\alpha = (\ln \frac{1-R}{T})/x \qquad (6)$$

In our experiments, T and R were measured at 77K and 300K on the Perkin-Elmer 621 IR Spectrophotometer in the wavelength range from 2.5 to 50 μm. In our transmittance measurements the effective thickness of the specimens was about 5 μm. The general view of the equipment used is presented in Figs. 13, 14, and 15.

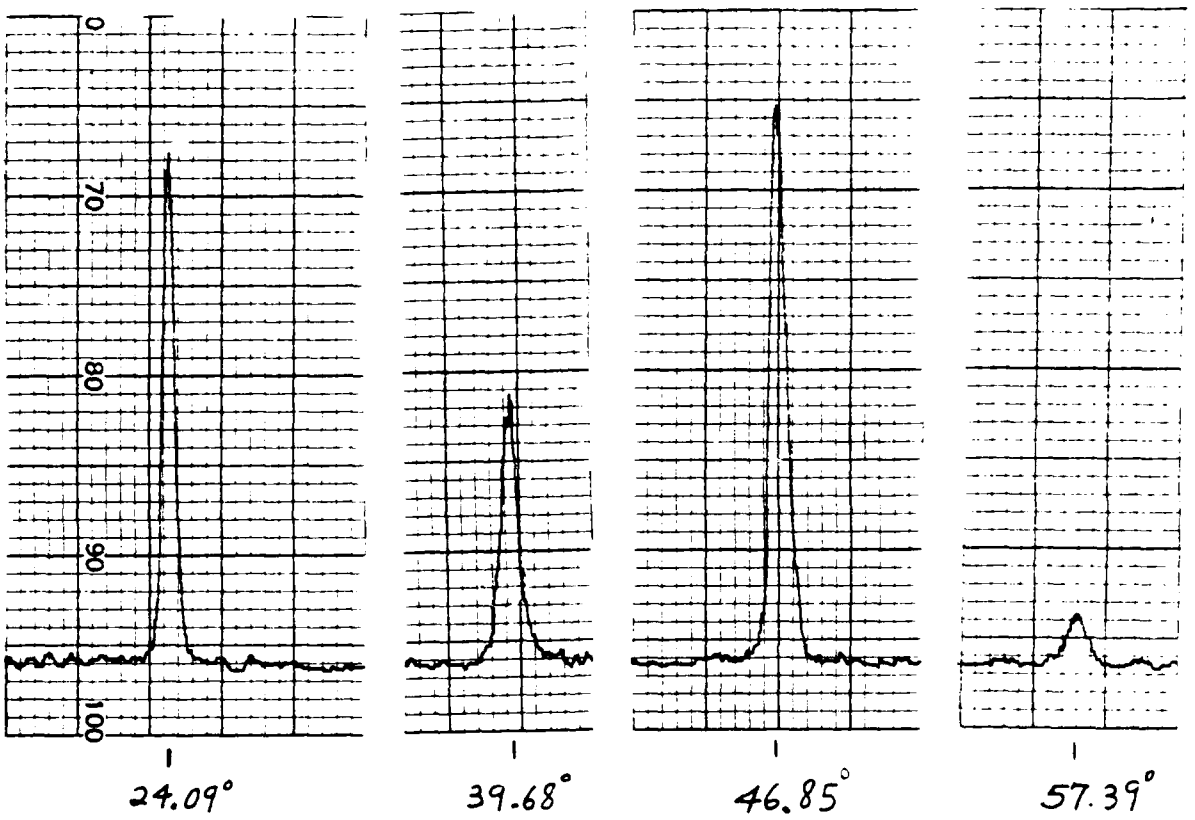

Fig. 10. An example of x-ray diffractogram
(90% InSb, 10% HgTe)

2.3. RESULTS

As was mentioned before, our main interest at this stage of investigation has been concentrated upon the samples with composition from 100% InSb to 75% InSb-25% HgTe, because of their energy gap. Another reason for this limitation is the fact that the pseudobinary section HgTe-InSb is a diagonal of a concentration rectangle $HgTe-In_2Te_3-InSb-Hg_3Sb_2$ that crosses the tetrahedron Hg-In-Sb-Te. Analysis of phases in the rectangle (which will be discussed in Section 3 of this report) provides reasons for the belief that solid solubility, along the diagonal and existence of the tetrahedral phases in the system HgTe-InSb, depends upon crystal structure of the individual phases in the pseudobinary systems $HgTe-In_2Te_3$, $InSb-In_2Te_3$, as well as in the practically unknown systems $InSb-Hg_3Sb_2$. But the fact that at least three out of the four mentioned compound have tetrahedral coordination (the crystal structure of Hg_3Sb_2 is unknown to the best of our knowledge) led us to assume that there is a wide region (or regions) of the tetrahedral phases in the quaternary system Hg-In-Sb-Te.

2.3.1. MICROSTRUCTURE

The synthesized ingots of solid solutions were dense and showed a metallic brightness. In a majority of the synthesis cycles, there were no deposits in the upper parts of the ampules. As already mentioned, the polycrystals had twins. The average size of a single-phase grain is within the limits of 0.5 to 3 mm. The series of photographs of the alloy microstructure is presented in Fig. 4.

Fig. 11. Varian Associates V6060 Magnet System used for Hall Effect measurements

2.3.2. MICROHARDNESS

It is known that the microhardness, H, of alloys, and particularly solid solutions (see, for example, [24]) is very sensitive to any variation in composition, and its measurement at different points of a sample can give a good estimation of compositional uniformity.

The results are presented in Table 4. One can see from the data that the microhardness dispersion is surprisingly small for polycrystals which indicates somewhat their uniformity. From the Table one can see that H reaches its maximum near the alloy with 10% HgTe. The shift of the maximum in the direction of InSb can be explained by the significant difference between H of the binary components (220 kgp/mm^2 for InSb[26] and 25 kgp/mm^{2}for HgTe [24]). For example, in the system HgTe-CdTe the maximum of H takes place near CdTe with the concentration of about 70 mole %, even the difference in H between CdTe ($\sim$42 kgp/mm^2) and HgTe is much smaller than in the system HgTe-InSb.

2.3.3. DTA DATA

In our experiments we used Barralls methodics [27], i.e. we measured endotherm onset temperature from the plot $\Delta T = \Delta T\ (T_{sample})$, where ΔT is the temperature difference between the sample and reference temperature. As already mentioned, tin was chosen as the reference material mainly because the magnitudes of specific heat for InSb and Sn (calculated per gram-atom) in accordance with the Dulong and Petit Law are practically the same (cf. atomic mass of Sn and average atomic mass of InSb).

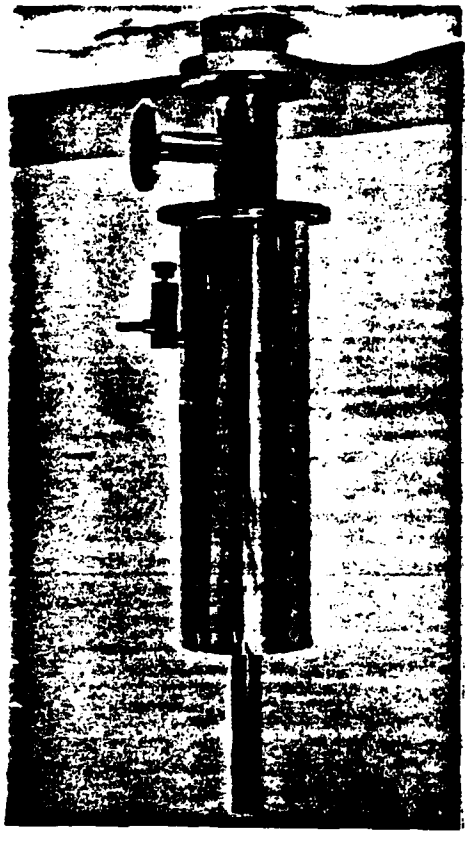

Fig. 12. Dewar used for measuring Hall effect at liquid helium temperature.

DTA curves for the samples of InSb used in our experiments* show a sharp effect related to the melting point 535°C, and a small but reproducible effect near 500°C. This effect relates, from our point of view, with nonstoichiometry of the InSb used. It has, apparently, an excess of antimony and the effect is a point on the eutectic line in the partial phase diagram InSb-Sb [28].

The DTA curve for an alloy with 2 mole % HgTe is typical for a solid solution with solidus and liquidus temperature close to 520 and 530°C, respectively. The points for the 5% HgTe alloy are close to 500 and 525°C. The 12, 15 and 20% alloys have solidus and liquidus points at 490 and 520°C, 480 and 515°C, 470 and 510°C, respectively. Reproducibility of the DTA data is ±10°C. The alloy with 35% HgTe is the most HgTe-rich solid solution we have produced so far. The almost vertical dashed line on the phase diagram is a presumable boundary between the area of solid solutions and eutectical alloys. But this conclusion may not be considered as a final one because the alloys with HgTe content greater than, say, 40 mole % are metastable ones.

The InSb-HgTe phase diagram based upon the results of our experiments is presented in Fig. 16. In accordance with the main goal of this project we have concentrated our attention upon the InSb-rich part of the system. While we had many runs of DTA for the left side of the diagram Fig. 16, the right side, as was mentioned before, presents only preliminary information.

*Average heating rate in our experiments was close to 3°C/min and the cooling is 1°C/min.

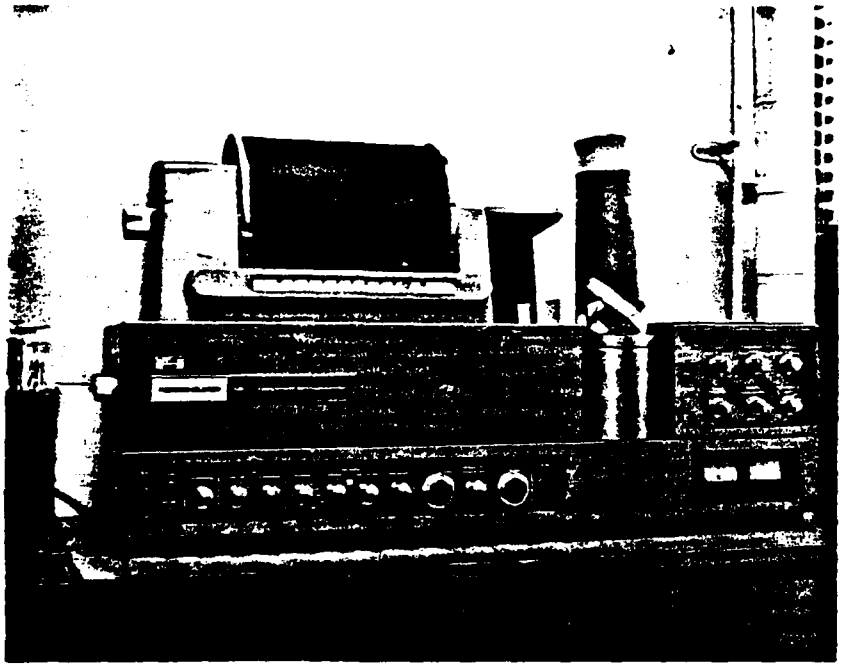

Fig. 13. Perkin-Elmer 621 Grating Infrared Spectrophotometer and the liquid nitrogen temperature optical dewar

The process of synthesis of the HgTe-rich alloys in the sealed ampules may be accompanied by decomposition of the binary component and even formation of new intermediate phases, e.g., In_2Te_3, Hg_3InTe_6, InTe, etc., depending on the thermochemical properties of these phases. To control these processes we ought to have an opportunity to control the magnitudes of partial pressure of the components of gas phase in the reaction volume. But it is a separate investigation that is not a part of this project.

From the phase diagram one can see that in the system InSb-HgTe, solid solutions exist in the range of HgTe concentration at least up to 35 mole % of HgTe. The means that we may change the absorption edge of the alloy in the wide range of magnitudes from 0.17eV to virtually zero (wave lengths greater than 7.3 um).

2.3.4. X-RAY DATA

The X-ray data are presented in Table 5. All samples of the solid solutions or the binary components have Miller's indices of zinc blend structure (space group $F\bar{4}3m$). With the chosen equipment and angles there are only four maximum peaks from the planes (111), (220), (311) and (400). Only for two specimens, 88% and 85% InSb, the maximum for (400) plane was not identified. One can see from the Table that this peak, for all samples, has a relatively small intensity. In a solid solution, the diffusive dispersion of the X-rays may be related to the difference in dispersion ability of the solid solution components.

TABLE 5. LATTICE PARAMETERS OF InSb, HgTe, AND $(HgTe)_x(InSb)_{1-x}$ FROM X-RAY DIFFRACTION VIA DEBYE METHOD.

Compound	θ(degrees)	peak intensity %	d_{hkl}(Å)	diamond-like (hkl)	a (Å)
	23.902	100.00	3.7197	111	6.4427
100%	39.443	77.55	2.2826	220	6.4562
InSb	46.599	31.82	1.9474	311	6.4588
	56.976	29.93	1.6149	400	6.4596
	23.823	100.00	3.7319	111	6.4638
98% InSb	39.372	64.66	2.2865	220	6.4672
2% HgTe	46.532	51.69	1.9500	311	6.4674
	56.881	18.03	1.6174	400	6.4696
	23.818	75.75	3.7325	111	6.4647
95% InSb	39.40	100.00	2.2845	220	6.4615
5% HgTe	46.552	66.15	1.9492	311	6.4648
	56.959	5.94	1.6152	400	6.4612
	24.092	70.68	3.6908	111	6.3927
90% InSb	39.684	57.37	2.2693	220	6.4185
10% HgTe	46.850	100.00	1.9375	311	6.4260
	57.387	12.41	1.6043	400	6.4172
	24.008	17.56	3.7034	111	6.4145
88% InSb	39.607	100.00	2.2735	220	6.4304
12% HgTe	46.858	12.63	1.9372	311	6.4250
	24.013	100.00	3.7028	111	6.4134
85% InSb	39.659	79.04	2.2706	220	6.4222
15% HgTe	46.881	52.06	1.9363	311	6.4220
	24.187	100.00	3.6765	111	6.3679
80% InSb	39.850	94.68	2.2602	220	6.3928
20% HgTe	47.050	40.28	1.9296	311	6.3998
	57.529	15.11	1.6007	400	6.4028
	24.074	100.00	3.6935	111	6.3973
100%	39.669	85.78	2.2701	220	6.4208
HgTe	46.836	58.34	1.9380	311	6.4276
	57.221	14.60	1.6085	400	6.4340

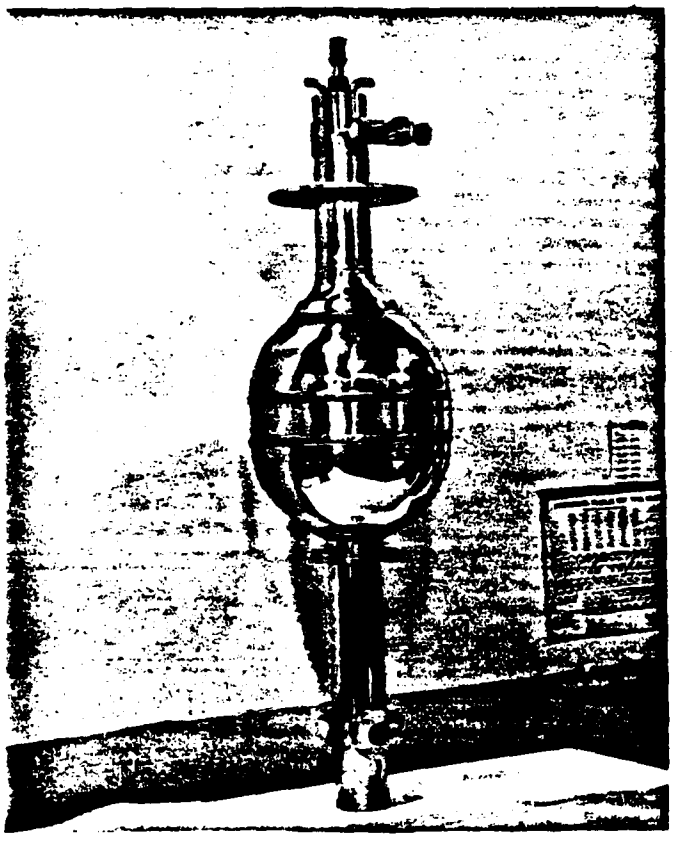

Fig. 14. Optical dewar used for measuring transmittance at liquid nitrogen temperature.

The composition dependence of the average lattice parameter, a, of the alloys is presented in Fig. 17. As could be predicted, there is a linear relation between a and the composition in the limits of existence of solid solutions.

2.3.5. SIGN, CONCENTRATION AND MOBILITY OF THE CURRENT CARRIERS

The type of conductivity was identified by the thermoelectric probe method (see, for example [29]). All investigated samples except HgTe have n-type conductivity. The measurements of conductivity and Hall effect were made at room temperature and at 77K. Our results showed that the differences in the magnitudes of carrier concentration and mobility at both of those temperatures were within the limits of experimental error. This could be expected for the semiconductors with $\varepsilon_g \leq 0.17$ eV, particulary for polycrystals. It is known (see, for example [30,31]), that even an n-type InSb single crystal with $n = 10^{17} cm^{-3}$ at $77^{o}K$ keeps this magnitude up to about 330K.

Measurements were undertaken on 13 samples with different shape (round and rectangular) and with different contact geometry. To receive more information from the galvanomagnetic measurements we also have made a series of magnetoresistance measurements. The averaged results of our measurements and calculations are presented in Table 6.

As it usually takes place in experiments on polycrystalline specimens, carrier concentration is relatively high and mobility is lower in comparison with their magnitudes in single crystals or epitaxial layers.

TABLE 6. THE AVERAGED RESULTS OF ELECTRICAL AND GALVANO-MAGNETIC MEASUREMENTS

Sample Composition (% mole)		$(\ \text{cm})^{-1}$	RH_3, cm/C	$n\ \text{cm}^{-3}$	μ_H, $\text{cm}^2/(\text{V.s}) \times 10^4$	
					from Hall data	from magneto-resistance data
InSb	HgTe					
100	-	2.2×10^{2}	2.8×10^{2}	2.2×10^{16}	6.3	5.1
95	5	1.1×10^{2}	2.4×10^{2}	2.6×10^{16}	2.6	1.8
90	10	2.3×10^{4}	2.8	2.2×10^{18}	6.5	2.1
85	15	6.0×10^{3}	2.2	2.9×10^{18}	1.2	3.8
80	20	3.6×10^{3}	1.1	5.7×10^{18}	3.9	2.5

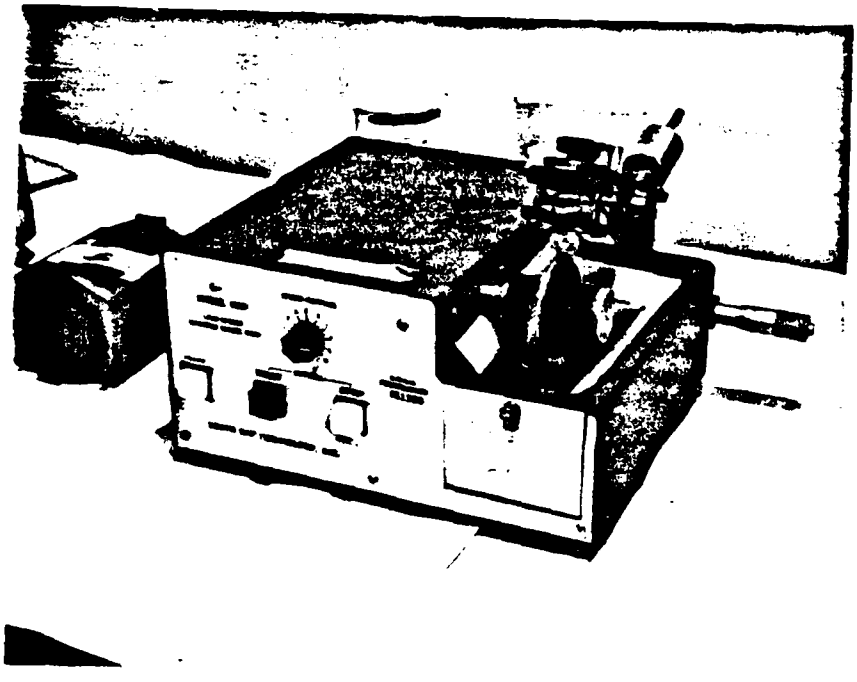

Fig. 15. Slow speed diamond wheel saw for preparation of slides of HgTe-InSb for optical measurements

2.3.6. OPTICAL MEASUREMENT DATA

The measurements of transmittance, T, and reflectance, R, provide relative magnitudes of T and R. To calculate the absorption coefficient and parameter $(\alpha hf)^2$ (see Eqns. 4 and 6, Sect. 2.2.6.) we have chosen several typical points on the experimental plots R ( ) and T ( ) and presented them in Table 7. The results of calculation of α and $(\alpha hf)^2$ are in the same Table. These data are used for the plots $hf = hf[(\alpha hf)^2]$, presented in Figures 18 to 23. Extrapolation of the straight linear parts of the plots to $(\alpha hf)^2 = 0$ gives the optical energy gap ε_g. Dependence of ε_g on the alloy composition is presented on Fig. 24. One can see that there is virtually linear dependence of ε_g on composition. There is a remarkable exception for the alloy $(HgTe)(InSb)_9$ whose ε_g is about 10% greater than an expected magnitude. We may explain it as the so-called Burstein shift [32] which consists of the optical absorption edge rise with increasing values of electron concentration. One can see from Table 6, Section 2.3.5. that conductivity of this alloy is greatest among the investigated compositions but the measured Hall electron concentration has the same order of magnitudes for half of the alloys. It gives us reason to assume that there is a strong compensation effect in the alloy and the real electron conncentration may be substantially greater than the measured magnitude. This effect was observed on InSb by Hrostovski et al. [33], Breckenridge et al. [34] and Kaiser et al. [35] for the crystals with n greater than $10^{18} cm^{-3}$.

TABLE 7. EXPERIMENTAL DATA OF THE TRANSMITTANCE AND REFLECTANCE MEASUREMENTS WITH THE RESULTS OF CALCULATION OF THE ABSORPTION COEFFICIENT.

Sample Composition %, (mole)		1/λ	hf	T	R	α	1-R	$(\alpha hf)^2$
InSb	HgTe	1/cm	eV	%	%	1/cm		
100	-	1500	0.186	20	47	1.9×10^3	53	1.24×10^5
		1250	0.155	25	45	1.6×10^3	55	6.2×10^4
		1000	0.124	34	40	1.1×10^3	60	1.9×10^4
		750	0.093	67	28	1.44×10^2	72	179
		650	0.081	80(max)	25(min)	0	75	-
		500	0.062	68	85	-	15	-
		1750	0.217	18	50	2.04×10^3	50	1.96×10^5
98	2	1750	0.217	26	31	1.95×10^3	69	1.8×10^4
		1500	0.186	28	29	1,860	71	1.2×10^4
		1250	0.155	35	23	1,577	77	6×10^4
		1000	0.124	70	12	458	88	3.2×10^3
		750	0.093	50	64	-	36	-
		925	0.115	90(max)	6	87	94(min)	100
95	5	1750	0.217	22	27	2343	71	2.5×10^4
		1500	0.186	24	26	2252	74	1.8×10^4
		1250	0.155	29	24	1926	76	8.9×10^4
		1000	0.124	48	19	1046	81	1.7×10^4
		800max	0.099	92	9	0	91	
		750	0.093	79	21	0	79	
90	10	1750	0.217	14	27	3303	73	5.14×10^5
		1500	0.186	17	26	2942	74	2.99×10^5
		1250	0.155	25	23	2250	77	1.21×10^5
		1000	0.124	56	18	763	82	8.9×10^3
		875max	0.109	85	13	46.5	87	25.7
		750	0.093	50	42	297	58	0.76×10^3
		500	0.062	12	77	1301	23	6.5×10^3
88	12	1750	0.217	20	32	2448	68	28×10^4
		1500	0.186	21	31	2379	69	20×10^4
		1250	0.155	23	30	2226	70	12×10^4
		1000	0.124	32	28	1622	72	4×10^4
		750max	0.093	90	21	-	79	-
		500	0.062	52	76	-	24	-
-	100	1750	0.217	3	40	5991	60	1.7×10^6
		1500	0.186	4	"	5416	"	1.0×10^6
		1250	0.155	5	"	4969	"	0.59×10^6
		1000	0.124	8	"	4029	"	0.25×10^6
		750	0.093	20	"	2197	"	0.042×10^6
		500	0.062	63	"	-	"	-
		400	0.050	81	"	-	"	-

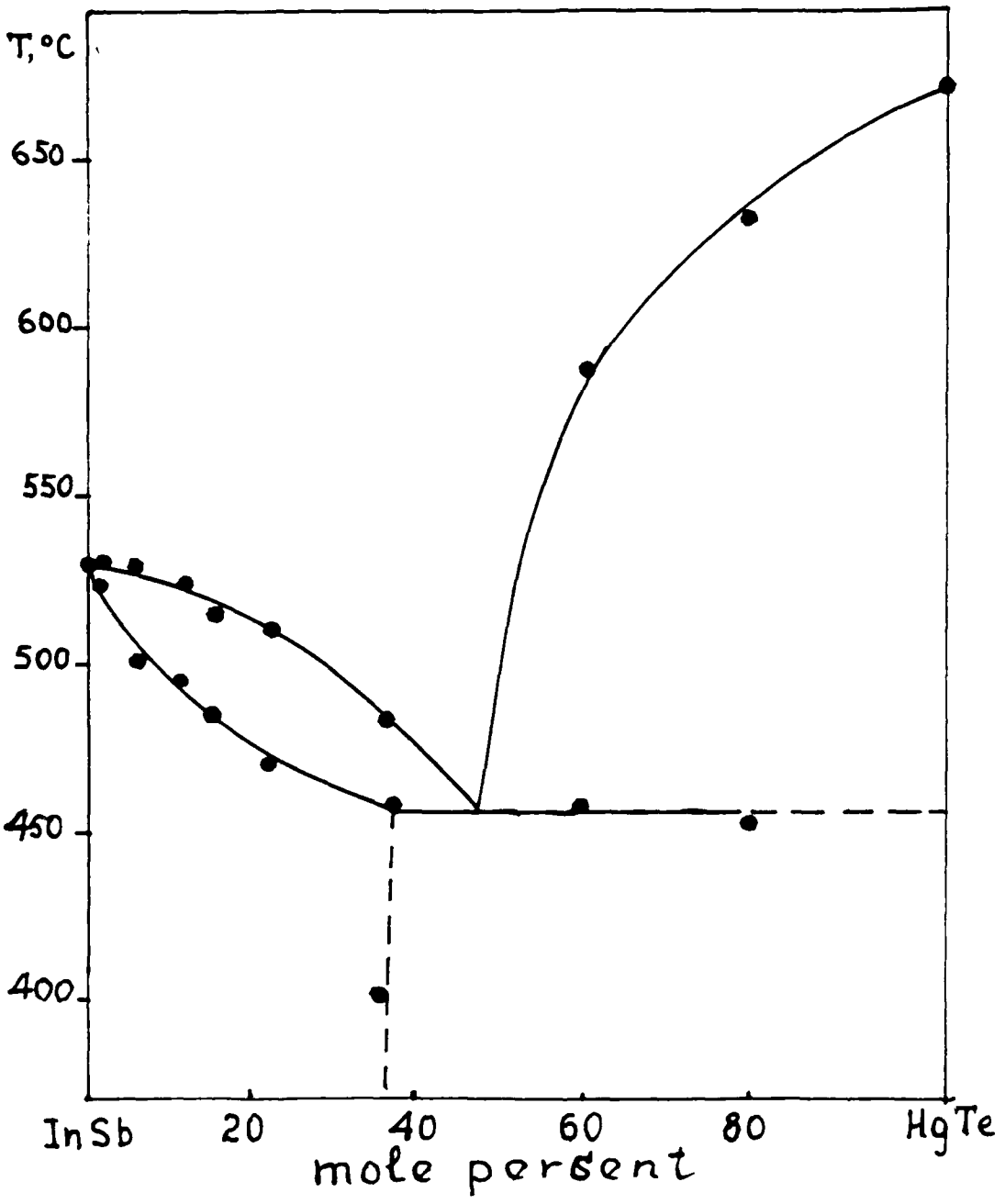

Fig. 16. Phase diagram of polycrystals of $(HgTe)_x(InSb)_{1-x}$

The curve for HgTe does not have a linear part that may be used for extrapolation. It may be connected with the fact that HgTe is a semimetal. The same effect we observed earlier while investigating some semiconductor phases with strong degradation [36].

3. ANALYSIS OF THE RESULTS

3.1. QUATERNARY SYSTEM Hg-In-Sb-Te

The system Hg-In-Sb-Te is interesting from both theoretical and practical points of view, because it consists of several regions that contain non-defect (InSb-based) and defect (In_2Te_3-based) tetrahedral, or diamond-like, semiconductors. The sides of the concentration tetrahedron (Fig. 25) contain altogether 12 compounds (both berthollides and daltonides) without taking into consideration the elemental components.

Our initial interest in this system was based upon the fact that each of the binary compounds HgTe and InSb have unlimited solubility in the solid state with the same compound InAs. This fact gives us some reason to expect that HgTe and InSb may create solid solutions in each other. The same approach was used before in the case of, for example, ZnSe and GaAs [37].

Tne binary system In-Sb [28,38] has only one compound InSb; system In-Te includes at least four phases: In_2Te, InTe, In_2Te_3 and In_2Te_5. The system Sb-Te includes the only phase Sb_2Te_3 which is interesting because of its variable composition (from 56 to 63 at. % Te). The phase Sb_2Te_3 has the hexagonal crystal lattice [39]. The system Hg-Te includes only one

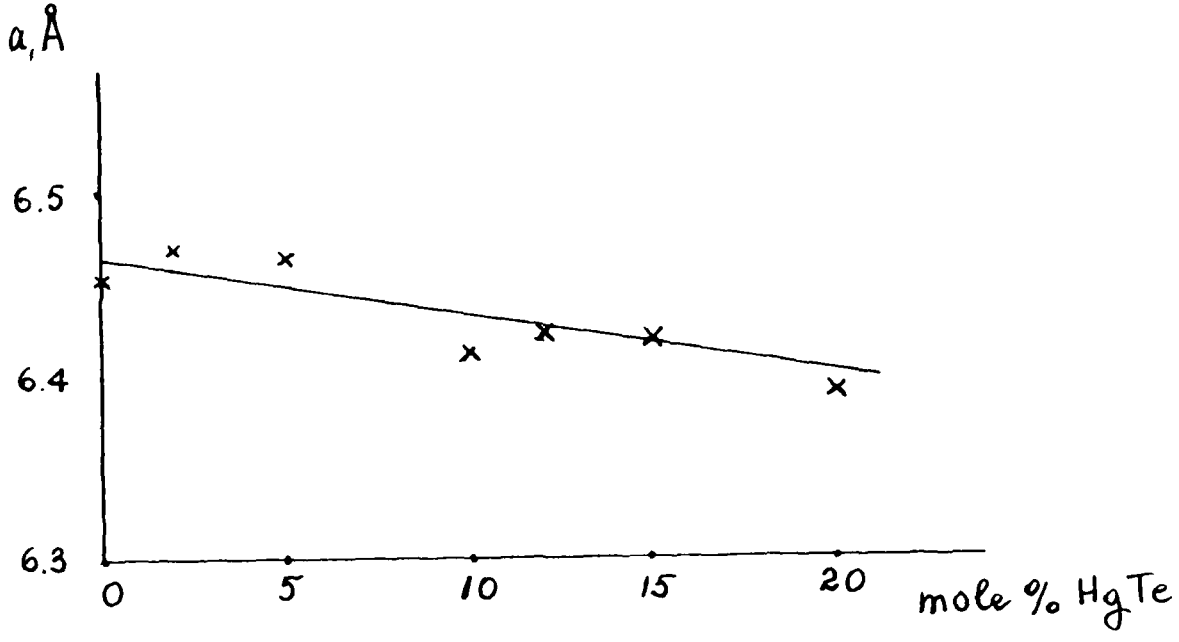

Fig. 17. Lattice parameter of alloy HgTe-InSb

compound HgTe. The system Hg-Sb has only one compound Hg_3Sb_2. This compound by far could not be prepared by metallurgical methods; it was synthesized by reaction of stibnine SbH_3 with mercuric chloride $HgCl_2$[40]. Binary system Hg-In includes one bertollide $HgIn_{11}$ that exists below 108°C and three low temperature phases Hg_6In, Hg_4In_3 and HgIn (melting points -14.2, -37.2 and -19.3°C, respectively).

3.2. Ternary Section HgTe-InSb-In_2Te_3

The most interesting part of the concentration tetrahedron Hg-In-Sb-Te from our point of view is a triangle HgTe-InSb-In_2Te_3. Some properties of these compounds are presented in Table 8.

The pseudobinary system In_3Sb_3-In_2Te_3 has solubility of In_2Te_3 in In_3Sb_3 up to 15 equimole percent [26,42]. The alloys have diamond-like crystal structure. The pseudobinary system Hg_3Te_3-In_2Te_3 [43,44] has a range of solid solutions from 100 to 50 equimole percent of HgTe, and another range of solid solutions on the In_2Te_3 base between 100 and 85 equimole percent In_2Te_3.

These literature data led us to expect that solubility exists also along the third side of the concentration triangle InSb-HgTe-In_2Te_3. The results of the first stage of our program have shown that the solubility exist at least up to 20 mole % of HgTe in InSb. As previously mentioned in our initial proposal for this project, the most interesting composition for practical use would be 85% InSb-15% HgTe; and we have the solid solution of this composition now among the other synthesized alloys.

TABLE 8. SOME PROPERTIES OF HgTe, InSb AND In_2Te_3 [26,41]

	HgTe	InSb	In_2Te_3
Crystal structure	Sphalerite	Sphalerite	Defect Sphalerite
Lattice parameter, A	6.4623 (Coloradorite)	6.47962(25°C) (6.47877)	6.16(600°C) 18.40(600°C, order)
Mol. mass, gram/mole	328.19	236.57	612.44
Ave. Atomic mass	164.10	118.29	122.49
Density, gram/cm	8.17	5.78	5.79
Microhardness, kgp/mm^2 (load: 50 p)	20	220	166
Melting point, °C	667	536	667
Thermal conductivity (R.T.) Cal/(cm.s.K)	-	4×10^{-2}	1.66×10^{-3}
Debye temperature, K	242	202	-
Minimum R. T. energy gap, eV	-0.15	0.165	1.0
Heat of formation, Kcal/mole	58	107	47.7
Mobility, cm^2/V.s. electrons	25000	78000	50
Holes	350	750	-
Dielectric constant	~21	15.7	-

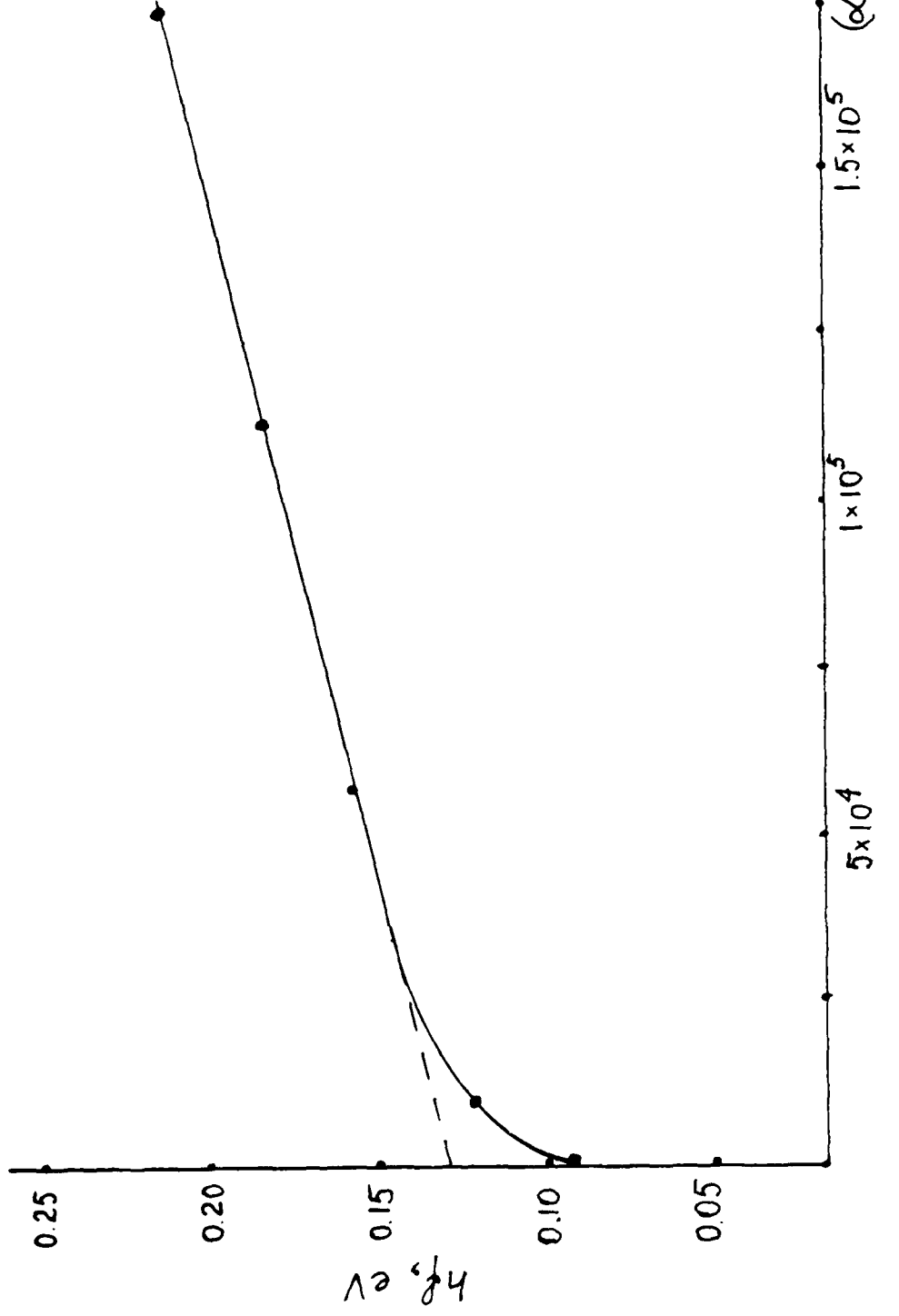

Fig. 18. The hf-$(\alpha hf)^2$ curve for InSb (300K).

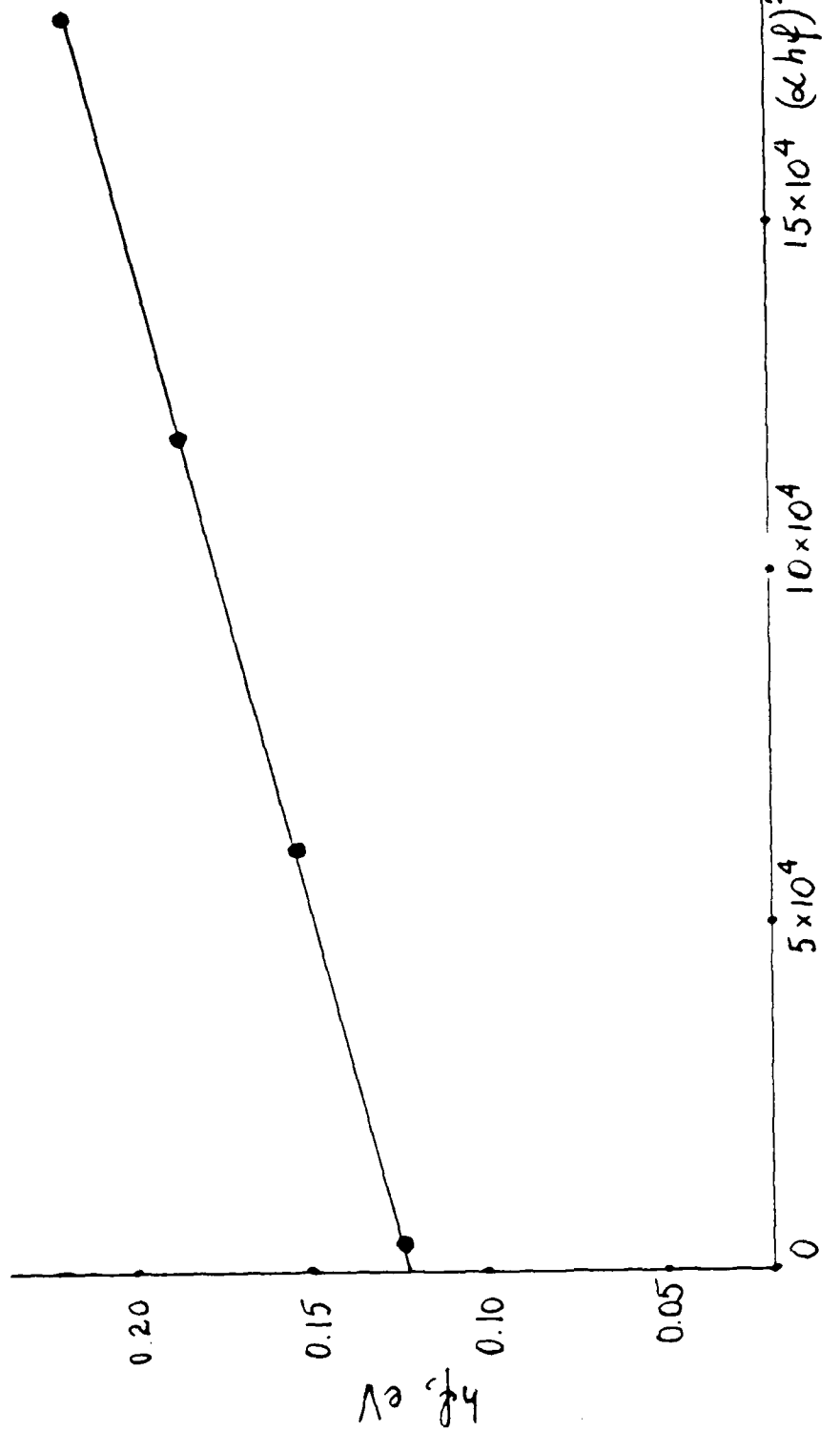

Fig. 19. The $hf-(\alpha hf)^2$ curve for 98InSb-2HgTe alloy.

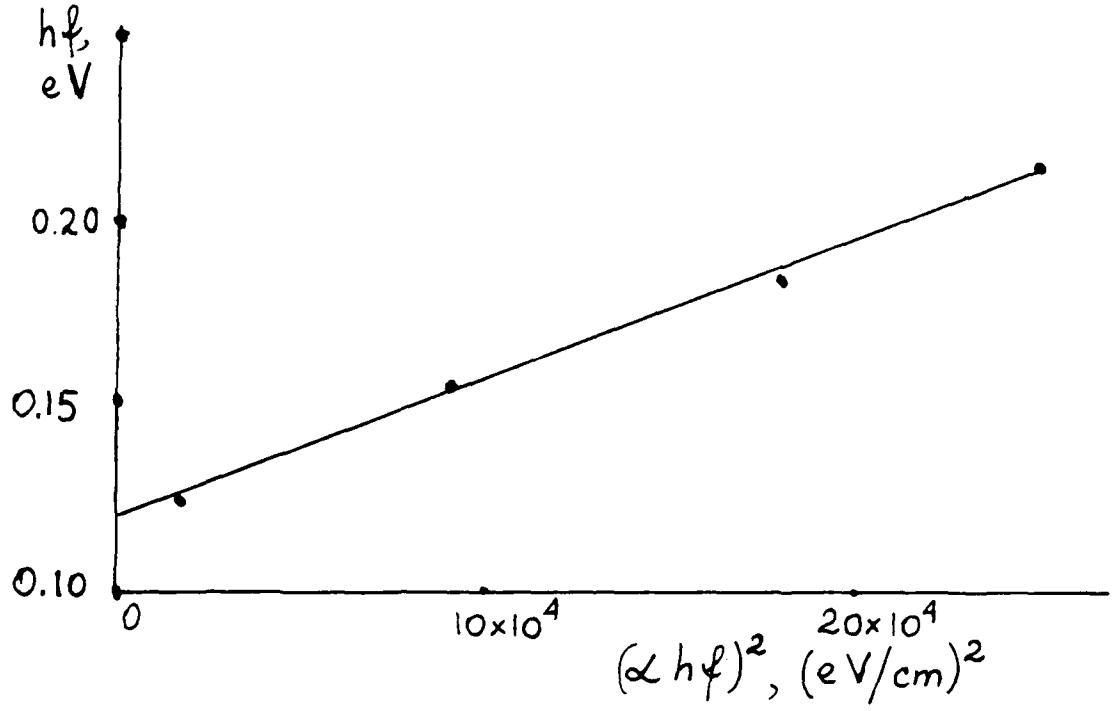

Fig. 20. The hf-$(\alpha hf)^2$ curve for 95InSb-5HgTe alloy.

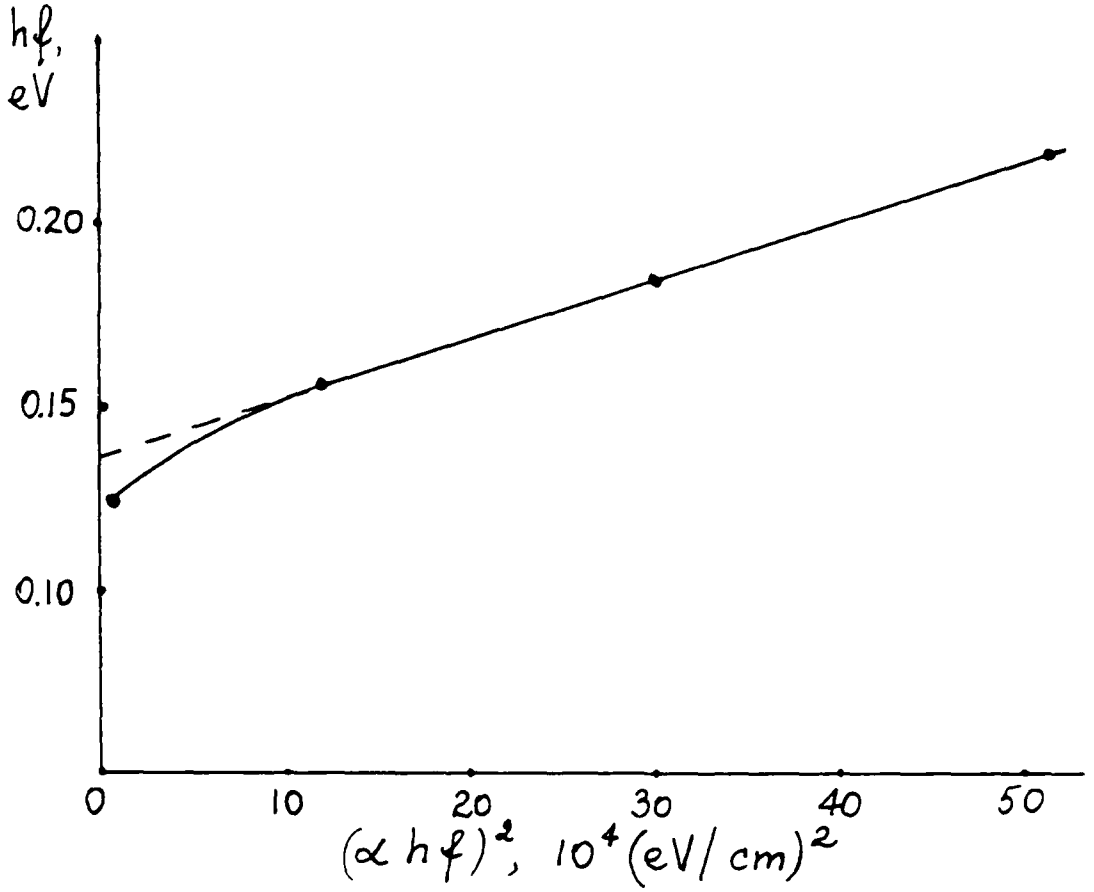

Fig. 21. The hf-$(\alpha hf)^2$ curve for 90InSb-10HgTe alloy.

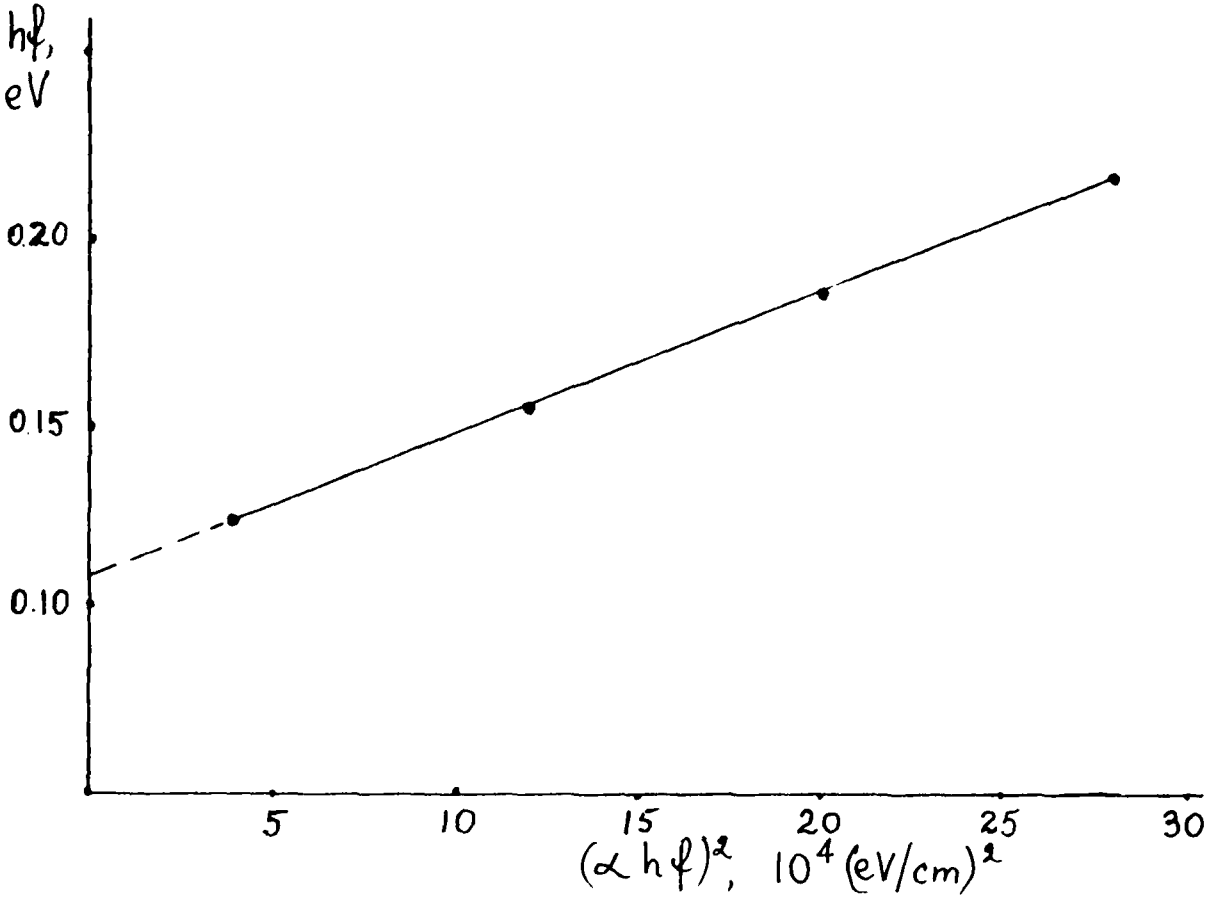

Fig. 22. The hf-$(\alpha hf)^2$ curve for 88InSb-12HgTe alloy.

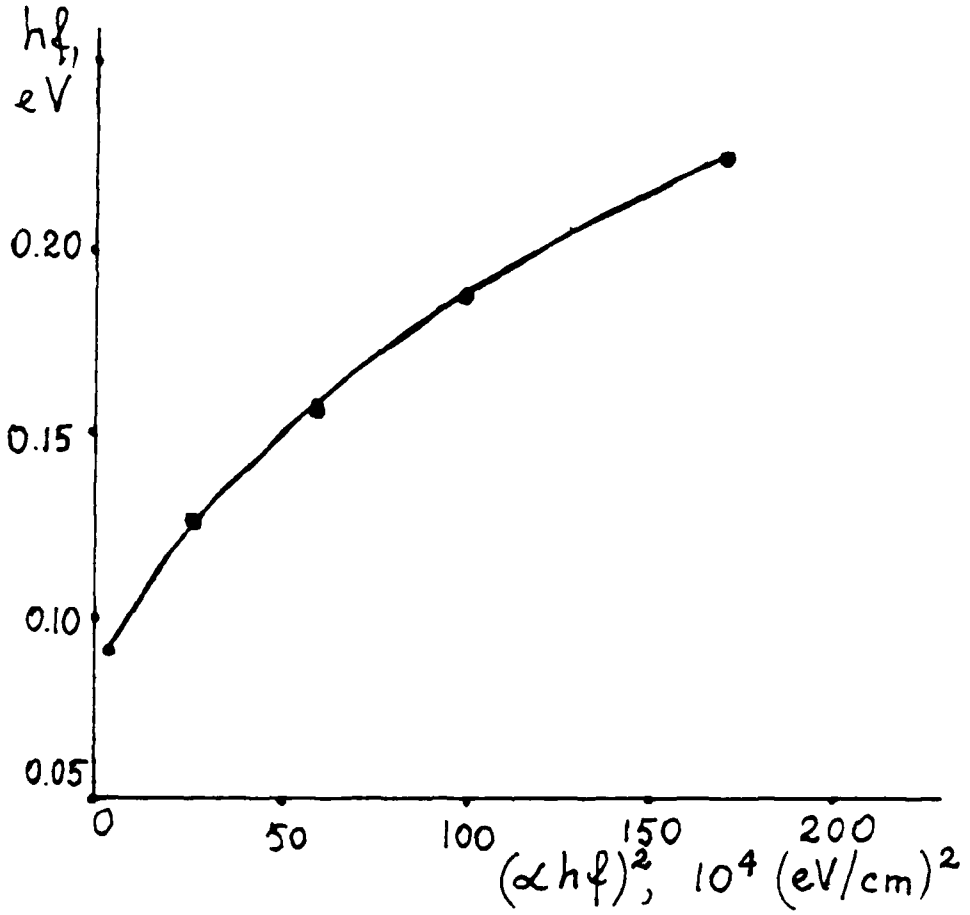

Fig. 23. The hf-$(\alpha hf)^2$ curve for a HgTe specimen.

3.3. ISOLVALENT AND HETEROVALENT SOLID SOLUTIONS OF THE BINARY II-VI AND III-V COMPOUNDS

The idea of preparation of solid solutions of semiconductors is very attractive because the solutions may have combinations of properties intermediate between the ones of the solution components. But, until now, all opportunities in this field have been far from their realization. The difficulties in the solid solution preparation relate to the predominant covalent interatomic interaction in the majority of II-VI and III-V compounds. This kind of interatomic bond is the cause of very slow diffusion which slowed down the process of reaching an equilibrium in crystal lattice. Very often, the DTA curves show effects connected to the nonequilibrium state of alloys, sometimes these effects imitate eutectic reactions in the alloy.

This nonequilibrium crystallization was initially mentioned in an early attempt to prepare solid solutions in the system Ge-Si[45]. Later, these effects were discovered in the systems III-V-III-V [46,47]. The same situation takes place in many II-VI-II-VI pseudobinary systems. In the case of these systems, the problem of the alloy homogenization is especially important for tellurides, and the main way to solve this problem, as one may conclude from the literature data, is a prolonged annealing.

Heterovalent solid solutions between III-V and II-VI compounds produce the same difficulties in the process of their homogenization, and the best way to prepare a homogenized ingot is the annealing at the temperatures as close to the solidus line as possible. The solidus line may be calculated

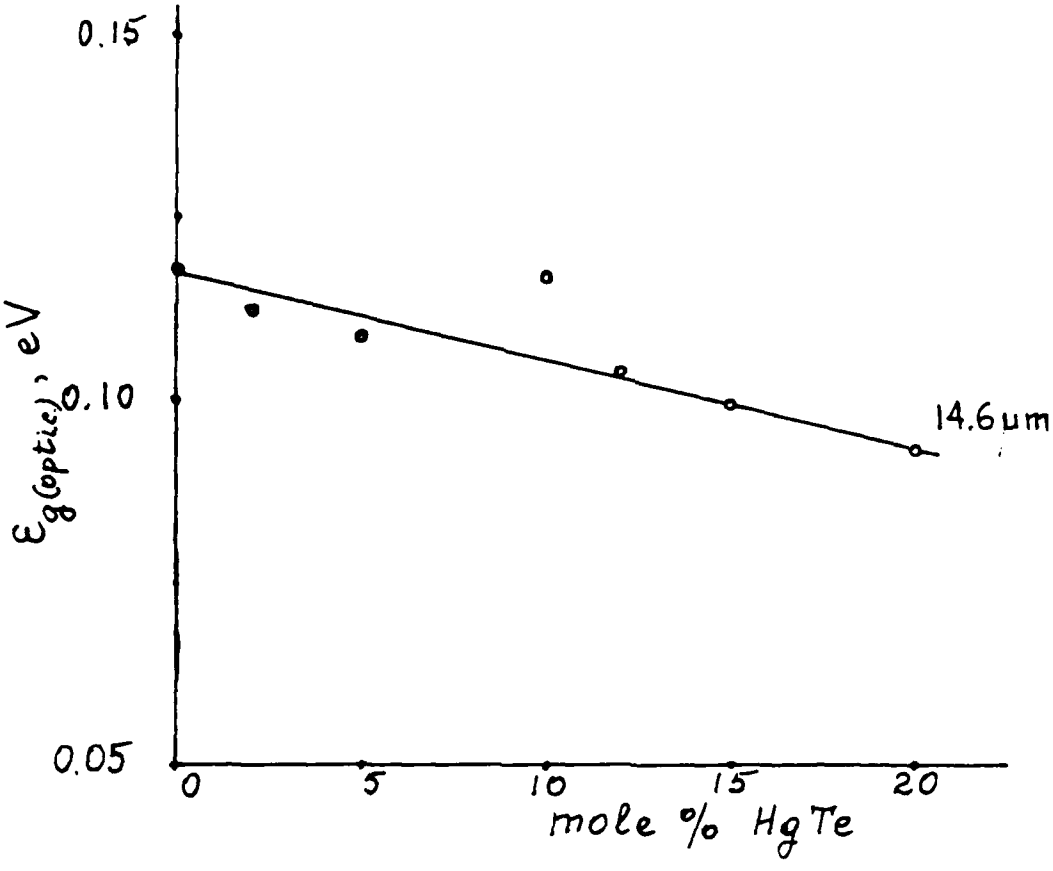

Fig. 24. Dependence of optical absorption edge on the alloy composition.

before-hand on the basis, for example, of the regular solution theory, or may be measured experimentally on the powder mixtures of the binary component homogenized by annealing.*

3.4. SECTION $HgTe-In_2Te_3-InSb-Hg_3Sb_2$ OF THE Hg-In-Sb-Te SYSTEM

A section of the concentration tetrahedron Hg-In-Sb-Te through the points HgTe, InSb and In_2Te_3 crosses the triangle In-Hg-Sb along the line $InSb-Hg_3Sb_2$ and the triangle Te-Hg-Sb along the line $HgTe-Hg_3Sb_2$ (see Fig. 26). In the tetrahedron we have a concentration rectangle $InSb-In_2Te_3-HgTe-Hg_3Sb_2$. The pseudobinary system HgTe-InSb which is a subject of our investigation is a diagonal of this rectangle. Analysis of phase composition in it may give us information about the area of existence of the tetrahedral alloys in the system Hg-In-Sb-Te. This may help in the solution of the technological problems in the growth of crystals or thin films with a definite set of parameters. The use of this approach was very fruitful in analysis of the quaternary systems In-Sb-Ga-As, In-Sb-Ga-P and In-As-Ga-P [49]. Apparently it makes sense to undertake an investigation of the alloys in the system $InSb-In_2Te_3-HgTe-Hg_3Sb_2$, but this might be the subject of a separate project.

*Annealing in powder gives an equilibrium alloy very fast but the sample cannot be used for investigation of electric and optical properties [48].

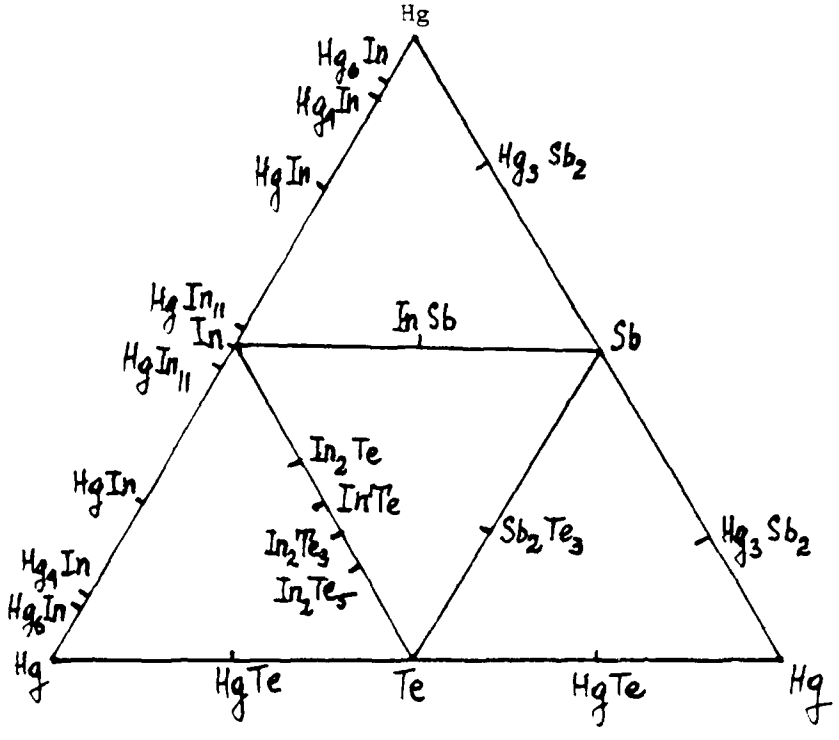

Fig. 25. The known phases in the quaternary system Hg-In-Sb-Te.

3.5. THE HgTe-InSb ALLOYS

3.5.1. PHASE DIAGRAM OF ALLOYS IN THE SYSTEM

The phase diagram (Fig. 16) reflects the results of DTA. As aforementioned, the presented diagram has to be considered as a first step in the investigation of phase equilibrium in the system of alloys. The data we have received on the alloys that are practically in equilibrium are in the range of HgTe content up to 20 mole %. This range includes all alloys whose optical absorption edge may present interest for their use in the infrared detectors.

We still believe that the results of DTA of the HgTe-rich alloys cannot be considered as ones reflecting the thermal effects in the state of equilibrium. This may be explained by the great magnitude of the covalent component of the interatomic bond in HgTe and uncontrollable sublimation and condensation of mercury atoms during a DTA run. It is possible that the difference in the energy of formation of InSb and HgTe has to be taken into consideration because this difference plays a different role with the change of the alloy composition. To check this possibility we have undertaken a four-cycle run of DTA (each cycle included heating and cooling of the specimen) on the sample 20% InSb-80% HgTe. All eight DTA curves have virtually the same shape. But we know (see, for example [50]), that the melting process takes away the effects of annealing and/or homogenization. Because of the results, it is reasonable to believe that homogenization was not reached in this sample, especially if we take into consideration the fact that mercury telluride itself decomposes starting

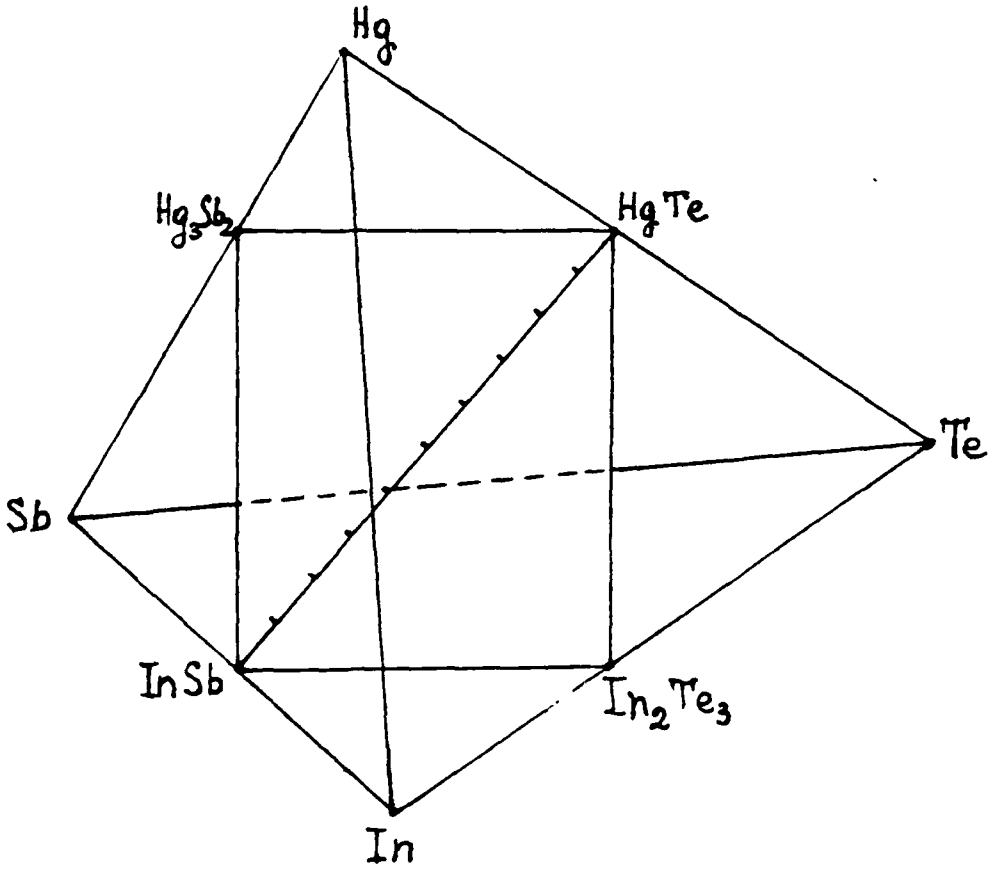

Fig. 26. Concentration tetrahedron Hg-Sb-In-Te. The rectangle $InSb-In_2Te_3-HgTe-(Hg_3Sb_2)$ is the area of possible existence of the diamond-like phases. The diagonal InSb-HgTe of the rectangle is the object of this project.

from about 500°C. This is why we conclude that the HgTe side of the HgTe-InSb alloy system requires a more detailed investigation that will have mainly theoretical interest because the HgTe-rich alloys do not belong to the group of IR-detector materials (in contrary with the HgCdTe alloys).

3.5.2. CRYSTAL STRUCTURE

One may see from Fig. 17 that composition dependence of the lattice parameter of the single phase alloys is practically linear which is common for solid solutions. This means that results of X-ray analysis prove the conclusions of microstructure analysis, the DTA data and results of microhardness measurements. Nonetheless we believe that X-ray investigation has to be repeated with analysis of diffraction on the angles closer to 180° to receive more accurate magnitudes of lattice constant. We are going to do this work on the polycrystals as well as on the single crystals we shall grow during the second year of this project. The accuracy of our current X-ray experiment is not adequate for the single crystals on films as may be seen from Fig. 17. If we extrapolate the plot to the composition 100% HgTe, the magnitude of lattice parameter will be smaller than the known one.

3.5.3. ELECTRICAL PROPERTIES

An important specific of the investigated polycrystals is that they have n-type conductivity for alloys of all composition except HgTe. This has led us to conclude that after a proper purification and single crystal growth, the sign of conductivity may be changed by doping or by inclination

from stoichiometry. We expect these materials may be used in photoresistive as well as in photovoltaic IR detectors. It is too early to draw a conclusion with regard to the composition dependence of the charge concentration and mobility, because the measurements were undertaken on the polycrystals. Nevertheless, relatively high magntidues of mobility provide proof for our initial supposition [52] regarding its high magnitudes for InSb-HgTe alloys. The small magnitude of electrical energy gap did not permit us to distinguish extrinsic and intrinsic parts of conductivity. To do so, we have to have more perfect single crystalline samples for measurements.

3.5.4. OPTICAL PROPERTIES

The results of the measurements of optical transmittance and reflectance showed that the absorption edge changes practically linearly with composition, and in accordance with our predictions. The concentration coefficient of the energy gap in the range 0-20 mole % HgTe is equal to -2.5×10^{-3} eV/percent. If we take for calculations ε_g InSb from our measurement, the composition of the alloy with $\varepsilon_g = 0$ will be about 50% HgTe. It is greater than a predicted magnitude (about 35% HgTe), but in our calculations there was an uncertainty about the effective thickness of the samples used for the transmittance measurement (about ±15%). If we correct our results by this factor, the experimental data will move to the higher magnitudes of ε_g in accordance with our prognostications. This kind of shift was observed, for example, in the investigation of optical properties of CdTe and CdS films [51].

4. SUMMARY

The investigations of the system $(HgTe)_x(InSb)_{1-x}$ have shown that solid solutions of the binary components exist at least in the range from x = 0 to x = 0.2. Measurements of the electrical, galvano-magnetic and optical properties have shown that the investigated single phase polycrystals are semiconductors with the linear dependence of energy gap on concentration.

Analysis of the experimental data and calculations on their basis have led us to conclude that the main goals of the first year of work on this project, namely

-evaluation of the range of solid solubility in the system,

-detailed physico-chemical analysis of the single phase polycrystals,

-evaluation of the principal electrical, galvano-magnetic and optical properties

have been achieved.

The results of this part of the investigation will be used in the next part of the project which includes primarily single crystal and expitaxial growth and characterization of the narrow-band $(HgTe)_x(InSb)_{1-x}$ semiconductors for far-infrared detectors.

5. ACKNOWLEDGEMENTS

The authors, Dr. L. I. Berger and Dr. S. W. Lin, wish to thank Dr. L. J. Burnett, Chairman of the Physics Department, Dr. S. B. W. Roeder, Chairman of the Chemistry Department, Dr. R. Bedore, Chairman of the Mechanical Engineering Department and Dr. P. Abbott, Chairman of the Geology Department of SDSU for the courteous opportunity to use department premises and equipment. We are grateful also to Mr. R. Steed for his help in optical measurements, and Ms. A. Sturz for the help in X-ray measurements. We express our appreciation to Dr. A. Clawson of Naval Ocean Systems Center, San Diego, for the opportunity of verifying our results of galvano-magnetic measurements on the NOSC equipment. We are especially grateful to the Office of the Naval Research for the financial support which makes this investigation possible.

6. REFERENCES

1. R. F. Brebrick and A. J. Strauss. J. Phys. Chem. Solids, 26, 989(1965).

2. J. E. Bowers, J. L. Schmit, C. J. Speerschneider, and R. B. Maciole K. IEEE Trans.; Electron Devices, ED-27, 24 (1980).

3. S. Sugawara, T. Sato, and T. Minamiyania. Bull. Jap. Soc. Mech. Eng. 5, 711 (1962).

4. L. I. Berger and E. G. Kotina. Inorg. Materials, 7, 2033 (1971).

5. R. T. Delves and B. Lewis. J. Phys. Chem. Solids, 24, 549 (1963).

6. H. Krebs, H. Weyand, M. Hancke. Z. Ange W. Chemie, 70, 468 (1958).

7. V. M. Glazov, S. N. Chizhevskaya. Soviet Phys. Solid State, 4, 1841 (1962).

8. W. J. Smothers, Chiang Yao. The Differential Thermal Analysis, N. Y. 1958.

9. A. Guinier, J. Tennevin. Acta crystallographica, 2, 133 (1949).

10. M. Rodot. Les Materiaux Semiconducteurs, Dunod, Paris, 1965.

11. M. Aven, J. C. Prener. Physics and Chemistry of II-VI Compounds. Wiley & Son. Amsterdam, New York, 1966.

12. H. W. Hayden, W. G. Moffatt and J. Wulff. The Structure and Properties of Materials, N. Y., John Wiley, 1965, Volume 3.

13. L. B. Valdes. Proc. IRE, 42, 420 (1954).

14. E. S. Meieran, J. Appl. Phys., 36, 3247 (1965).

15. D. K. Hamilton and K. G. Seidensticker. J. Appl. Phys. 34, 2697 (1963). See also: V. M. Glazov, S. N. Chizhevskaya and N. N. Glagoleva, Liquid Semiconductors. Moscow, Publ. House "Nauka", 1967 (p. 87) (in Russian).

16. A. F. Frederickson. Am. Mineral 39, 1023 (1954). See also: B. W. Neate, D. Elwell, S. H. Smith and M. D'Agostino. J. Phys. E. 4, 775 (1971)

17. H. G. McAdie. Proc. 3rd Intern. Conf. for Thermal Analysis, V. 1, Birkhauser Verlag, Basel, 1972, p. 591; See also: NBS-ICTA Standard Ref. Mat. 758.

18. See: NBS Circular #500, Part 1, 1952.

19. R. E. Bolz and G. L. Tuve (Ed.) Handb. Tables Appl. Engr. Science CRC Publ., 1970.

20. L. J. Van der Pauw. Philips Res. Reports 16, 187(1961); Ibid., 13, 1(1958); Philips Tech. Rev., 20, 220(1958).

21. J. Kudman, T. Seidel. J. Appl. Phys., 33, 771(1962).

22. E. D. Palik and D. L. Mitchel, in Physics of Solids in Intense Magnetic Fields, Plenuum Publ. Corp. 1969 (p. 90).

23. F. Bassani and G. P. Parravicini. Electronic States and Optical Transitions in Solids. Pergamon Press (1975).

24. B. B. Sharma, S. K. Mehta and V. V. Agashe. Physica Status Sol. A60, K105 (1980).

25. V. M. Glazov and V. N. Vigdorovich. Microhardness of Metals and Semiconductors. Plenum, N.Y., 1971.

26. N. A. Goryunova. Multicomponent Diamond-like Semiconductors. Plenum, N.Y., 1969.

27. E. M. Barral. Thermochim. Acta, 5, 377 (1973).

28. P. Hansen. Constitution of Binary Alloy, McGraw-Hill, N.Y., 1958 (p. 859).

29. L. J. Kroko, A. G. Milnes. Solid State Electronics, 8, 829 (1965).

30. H. Fritzsche. Phys. Rev. 120, 1120 (1960).

31. J. A. Van Vechten. Handbk. of Semiconductors. Vol. 3, North Holland, Amsterdam, 1980 (p. 1).

32. E. Burstein. Phys. Rev. 93, 632 (1954).

33. H. J. Hrostowski, G. H. Wheatley, W. F. Flood. Phys. Rev. 95, 1683 (1954).

34. R. G. Breckenridge, R. F. Blunt, W. R. Hostler, H. P. R. Frederikse, J. M. Becker, W. Osinsky. Phys. Rev. 96, 571 (1954).

35. W. Kaiser, H. Y. Fan. Phys. Rev. 98, 966 (1955).

36. V. M. Petrov, A. E. Balanevskaya, F. F. Kharakhorin, L. I. Berger. Inorg. Materials. 2, 1874 (1966).

37. N. A. Goryunova, N. N. Fedorova. Sov. Phys. Solid State, 1, 344 (1959).

38. F. A. Shunk. Constitution of Binary Alloys, Second Supplement. McGraw Hill, 1969.

39. E. Donges. Zs. Anorg. Chem. 265, 56(1951).

40. Y. A. Ugai and V. L. Gordin. Rus. J. Inorganic Chem. 7, 360 (1962).

41. B. P. Pamplin in Handbk. of Chemistry and Physics, 64th Ed., CRC Press 1983-84 (p. E-92).

42. D. L. Greenaway and M. Cardona. Proc. Int. Conf. Phys. Semiconductors, Exeter, 1966 (p. 666).

43. A. M. Spencer. Brit. J. Appl. Phys., 15, 625 (1964).

44. B. Ray and A. M. Spencer. Solid State Comm., 3, 389 (1965).

45. H. Stohr and W. Klemm. Zs. Anorg. Allg. Chem. 241, 305(1939).

46. C. Shih and E. A. Peretti. J. Amer. Chem. Soc., 75, 608(1953).

47. W. Koster and B. Thoma. Zs. Metallkunde, 46, 293(1955).

48. N. A. Goryunova, N.N. Fedorova. Soviet Physics. Techn. Physics. 25, 1339(1955).

49. E. K. Muller, J. L. Richards. J. Appl. Phys. 35, 1233(1964).

50. S. D. Raevskii, K. R. Zbigli, G. F. Kazak and M. D. Prunich. Inorg. Materials. 19, 889(1983).

51. H. Sitter, J. Humenberger, W. Huber and A. Lopez-Otero. Solar Energy Materials 9, 199 (1983).

52. L. I. Berger, Abstracts of Fifth Internat. Conf. on Vapor Growth and Epitaxy/Fifth American Conf. on Crystal Growth, San Diego, July 19-24, 1981 (page 331).

END

FILMED

2-85

DTIC